Models for left-right multiplicities*

Dennis Sivers
Stanford Linear Accelerator Center, Stanford University, Stanford, California 94305

Gerald H. Thomas
High Energy Physics Division, Argonne National Laboratory, Argonne, Illinois 60439
(Received 21 September 1973)

In the context of various models for production processes, we examine what can be learned from data on the number of charged particles per event in the left and right c.m. hemispheres, left-right multiplicity distributions. The appropriate generating-functional formalism is developed. We make explicit calculations of the generating function in both the multiperipheral and Mueller-Regge approaches. We explain how left-right multiplicity distributions are used to separate the components of a hybrid (diffraction plus short-range-order) model. Questions concerning the factorization of the leading Regge singularity are also discussed.

I. INTRODUCTION

Recent data from the National Accelerator Laboratory (NAL), from the CERN Intersecting Storage Rings (ISR), and from the Serpukhov machine have stimulated an active interest in building models for charged-particle multiplicity distributions as well as for one- and two-particle inclusive distributions.[1-3] The inclusive distributions are of interest theoretically because, as shown by Mueller,[4] they give direct information about Regge singularities through a generalized optical theorem. Moreover, the constraints

$$\langle n\rangle = \int \rho_1(\vec{p}, s)\frac{d^3p}{E}, \tag{1.1a}$$

$$\langle n(n-1)\rangle - \langle n\rangle^2 = \int C_2(\vec{p}_1, \vec{p}_2, s)\frac{d^3p_1}{E_1}\frac{d^3p_2}{E_2}, \tag{1.1b}$$

etc., relate the moments of the multiplicity distribution to the inclusive distributions and correlation functions.

Multiplicity distributions have proved useful in testing general theoretical pictures of hadron scattering, but since several different shapes of correlation function can have the same integral it is important to move toward more finely grained distributions. At the same time, for data of limited statistics there is an obvious advantage to studying integrated quantities. An interesting compromise between completely integrated and completely differential measurements consists of determining the number of particles (which in practice are charged) going left ("backward") and going right ("forward") in the center-of-mass system. Data of this type will be referred to as left-right multiplicity (LRM) distributions, $\sigma(n_L, n_R)$. From these data, more refined information about inclusive distributions is obtained than in Eq. (1.1):

$$\langle n_L\rangle = \int_{p_L<0}\frac{d^3p}{E}\rho_1(\vec{p}, s), \tag{1.2a}$$

$$\langle n_L n_R\rangle - \langle n_L\rangle\langle n_R\rangle = \int_{p_{L1}<0}\frac{d^3p_1}{E_1} \times \int_{p_{L2}>0}\frac{d^3p_2}{E_2}C_2(\vec{p}_1, \vec{p}_2, s), \tag{1.2b}$$

etc.

Left-right multiplicity distributions are extremely easy to obtain in bubble chamber experiments and many types of counter experiments. What we would like to show here is that LRM distributions already contain enough information to answer some crucial questions about the dynamics of production processes.[5,6] In particular, they provide a series of quantitative tests for the factorization of the leading Regge singularity.[7] These tests will be reviewed in Sec. II along with a discussion of the meaning and content of factorization. For completeness, an introduction to the generating-function formalism is included.[8] This formalism is convenient for the discussion of these multiplicity distributions and the closely related question of charge transfer across c.m. hemispheres. Differences between charged multiplicities and total multiplicities are discussed in this section as well.

To supply concrete examples of what can be learned from LRM, we turn in Sec. III to model calculations. Two main classes of models are distinguished: those constructed directly for inclusive distributions and those constructed directly for exclusive distributions. Inclusive models use the Mueller-Regge ideas; exclusive models are constructed, for the most part, using the multiperipheral picture, although adaptations of the multiperipheral picture to include diffraction are discussed as well. In addition, the Bjorken-

Feynman-Wilson fluid analogy is here considered as a simple reformulation and extension of the multiperipheral picture. In discussions we shall loosely include all three of these exclusive classes of models in the "multiperipheral picture." Separate from this multiperipheral picture is the fragmentation picture. We discuss some simple predictions of this approach, but since recent data seem to discredit it as an explanation for data in the central region[9] we will not present detailed calculations.

The model of Frazer, Peccei, Pinsky, and Tan[3(f)] (FPPT) is chosen as a representative example of a model formulated directly in terms of inclusive multiplicity moments. The one-dimensional version of the multiperipheral model due to DeTar,[10] the "nearest-neighbor multiperipheral model" (NNMM), gives an easily understandable introduction to the multiperipheral picture. We give a summary of the relevant details of this model, as well as generalizations. These generalizations include (1) the extension to two-pole multiperipheral models which give, in certain approximations, a nonfactorizing hybrid or "two-component"[11] model; and (2) an exactly calculable model of Kac, Uhlenbeck, and Hemmer[12] (KUH) which may have some relevance to the problem of understanding the effects of final-state interactions in high-energy data. This latter model is only one of a large class of fluid models which can be treated in a "mean-field approximation." The consequences of such an approximation are also presented.[13]

In Sec. IV, we apply what we have learned to the available data on left-right multiplicities and to the related quantity charge transfer. The claim[7] that data on $\sigma(n_L, \text{tot})$ at 205 GeV/c provide direct evidence for a diffractive or fragmentation mechanism is examined in more detail, and the possibility of separating out the fraction of events which correspond to diffractive fragmentation is discussed. Data on $\langle n_L\rangle_R$ vs n_R at current energies are shown to favor a situation in which the left-right cross sections do not factorize, although the situation is not clear-cut. Finally, we show that data on charge transfer in pp collisions can give some information on the size of the corrections to factorization.

II. GENERAL CONSIDERATIONS AND GENERATING-FUNCTION TECHNIQUES

The generating-function formalism has proved to be an exceptionally valuable tool for dealing with multiplicity distributions in hadronic production processes.[8] In this section we introduce the notation that we will use for the generating function, and define in terms of this function what we mean by inclusive, exclusive, or "mixed" quantities. Many of the results in this section are contained in a previous paper.[7] The treatment here is made more general so that in addition to left-right multiplicities, the related question of charge transfer can be discussed. The various experimental quantities we discuss are indicated in Table I.

A. Notation

It may make our later definitions clearer if we give first a simple example of a generating function in terms of the cross section $\sigma(n, s)$ for producing n particles. Given the complete set $\{\sigma(n, s)\}$ at a given c.m. energy $\sqrt{s}$, the function of the parameter z,

$$Q(z, s) \equiv \sum_n \sigma(n, s) z^n \,, \tag{2.1a}$$

is formed. Clearly all the information contained in $\{\sigma(n, s)\}$ is contained in the function $Q(z, s)$. In fact, $\sigma(n, s)$ can be recovered using

$$\sigma(n, s) = \frac{1}{n!} Q^{(n)}(0, s) \,, \tag{2.1b}$$

where $Q^{(n)}(z, s) = (\partial^n/\partial z^n) Q(z, s)$. The advantage of the generating function is that inclusive moments can also be simply obtained:

$$f_m(s) = \frac{1}{m!} \frac{\partial^m}{\partial z^m} \ln Q(z, s)\Big|_{z=1} \,, \tag{2.1c}$$

where it is easy to check that

$$\begin{aligned} f_1(s) &= \langle n\rangle \,, \\ f_2(s) &= \langle n(n-1)\rangle - \langle n\rangle^2 \,, \end{aligned} \tag{2.1d}$$

etc. The definition we will use for *exclusive* quantities will correspond to the situation (2.1b), where Q and its derivatives are evaluated at $z = 0$; *inclusive* quantities arise from (2.1c), where Q and its derivatives are evaluated at $z = 1$. If we distinguish between particles either by quantum number or by binning events in different kinematic regions so that more than one type of z will be present in Q, then the possibility of "mixed" quantities exists, where some z's are unity and the remainder are zero.

A typical example of a mixed quantity is the cross section $\sigma(n_{\text{ch}}, s)$, where n_{ch} represents the number of charged particles and a sum is taken over the unseen neutrals. Such mixed quantities are also frequently called semi-inclusive.

These expressions for the integrated quantities $\sigma(n, s)$ and $f_m(s)$ correspond to the usual definitions. The $\sigma(n, s)$ are integrals over the exclusive differential cross section

TABLE I. Table of measurable experimental quantities. "Coarse-grained" quantities are integrals ("sums") over fine-grained quantities, averages over kinematic variables. "Inclusive" quantities are sums over exclusive quantities, averages over (unseen particles) channels. Everything is tied together by a generating functional.

	"Coarse-grained" integrated quantities	Increasing momentum resolution →	"Fine-grained" differential quantities
Inclusive quantities	σ_{tot}	$\langle n_L\rangle$, $\langle n_L n_R\rangle$	$\rho(y_1)$, dQ/dy
	$\langle n_{\text{ch}}\rangle$, $\langle n_{\text{ch}}(n_{\text{ch}}-1)\rangle$	$\langle\langle u^2\rangle\rangle$	$C(y_1,y_2)$
Mixed semi-inclusive quantities		$\langle u^2\rangle_{n_R}$	
		$\langle n_L\rangle_{n_R}$	$\rho(y_1)\vert_{n_{\text{ch}}}$
	$\langle n_0\rangle_{n_-}$, $\langle n_K\rangle_{n-}$	$\sigma(n_L,\text{tot})$	
	$\sigma(n_{\text{ch}})$	$\sigma(n_L,n_R)$	$\sigma(n_L,n_C,n_R)$
			for example,
		$\sigma(n_L,n_R,u)$	3 momentum bins
			$\dfrac{d\sigma(y_1\cdots y_n)}{dy_1\cdots dy_n}$
Exclusive quantities	$\sigma(n_+,n_-,n_0)$	$\sigma(n_{+L},n_{-L},n_{0L};n_{+R},n_{-R},n_{0R})$	No. bins $\gg n_{\max}$
	1 momentum bin	2 momentum bins	...

$$\frac{d\sigma_n}{(d^3p_1/E_1)\cdots(d^3p_n/E_n)}$$

for producing exactly n particles (treated here as identical). The $f_m(s)$ are integrals over the inclusive correlation functions $C_m(\vec{p}_1,\ldots,\vec{p}_m)$, where

$$\sigma(s)=\sum_n \sigma(n,s)\,,$$

$$\rho_1(\vec{p}_1,s)=\frac{1}{\sigma(s)}\sum_n\frac{d\sigma_n}{d^3p_1/E_1}\,, \tag{2.1e}$$

$$\rho_2(\vec{p}_1,\vec{p}_2,s)=\frac{1}{\sigma(s)}\sum_n\frac{d\sigma_n}{(d^3p_1/E_1)(d^3p_2/E_2)}\,,$$

$$C_2(\vec{p}_1,\vec{p}_2,s)=\rho_2(\vec{p}_1,\vec{p}_2,s)-\rho_1(\vec{p}_1,s)\rho_1(\vec{p}_2,s), \tag{2.1f}$$

etc.

It is an interesting exercise to take one step from completely integrated quantities toward differential cross sections by imagining an experiment with exactly two momentum bins. In this case we will assume that each bin consists of an entire hemisphere in the c.m. system centered around the beam or target directions. To discuss the production of charged particles in the left and right c.m. hemispheres, we form the generating function

$$Q(z_{+L},z_{-L},z_{+R},z_{-L},s)=\sum\sigma(n_{+L},n_{-L},n_{+R},n_{-L},s)\times z_{+L}^{\,n_{+L}}z_{-L}^{\,n_{-L}}z_{+R}^{\,n_{+R}}z_{-R}^{\,n_{-R}}\,; \tag{2.2}$$

the summation here, and in what follows, goes over all values of those n's appearing in the summand. The notation is self-evident; $n_{\pm L}$ is the number of "±" particles in the left ("backward") and $n_{\pm R}$ the number in the right ("forward") hemisphere. We assume a sum over the unseen neutral particles: They can be explicitly included, if needed, by introducing the extra factors $z_{0L}^{\,n_{0L}}z_{0R}^{\,n_{0R}}$ with the completely exclusive cross sections

$$\sigma(n_{+L},n_{-L},n_{0L};n_{+R},n_{-R},n_{0L})$$

inside the summation (2.2).

Because of charge conservation, the four n's in (2.2) are not independent. A smaller set is

$$n_L=n_{+L}+n_{-L}\,, \tag{2.3a}$$

$$n_R=n_{+R}+n_{-R}\,, \tag{2.3b}$$

$$u=\tfrac{1}{2}[(n_{+R}-n_{-R})-(n_{+L}-n_{-L})]-\tfrac{1}{2}(q_a-q_b)\,, \tag{2.3c}$$

where n_L is the number of charged particles in the left hemisphere, n_R the number in the right hemisphere, and u the net charge transfer from the

right to the left. Here q_a and q_b are the charges of the initial particles. Charge conservation eliminates one n_i from the original set through the constraint

$$q_a+q_b=(n_{+L}+n_{+R})-(n_{-L}+n_{-R})\ . \tag{2.3d}$$

Thus (2.3c) can be written equivalently as

$$\begin{aligned} u&=n_{+R}-n_{-R}-q_a \\ &=n_{-L}-n_{+L}+q_b\ . \end{aligned} \tag{2.3c$'$}$$

The set (2.3) suggests introducing a new set of variables into the generating function:

$$\begin{aligned} &z_L=(z_{+L}z_{-L})^{1/2}\ , \qquad z_R=(z_{+R}z_{-R})^{1/2}\ , \\ &x=\left(\frac{z_{+R}z_{-L}}{z_{+L}z_{-R}}\right)^{1/2}\ , \qquad x'=\left(\frac{z_{+L}z_{+R}}{z_{-L}z_{-R}}\right)^{1/2} \end{aligned} \tag{2.4}$$

Note that $xx'=z_{+R}/z_{-R}$ depends only on "right" quantities and $x'/x=z_{+L}/z_{-L}$ depends only on "left" quantities. In terms of Eq. (2.4), (2.2) becomes

$$\begin{aligned} &Q(z_{+L}, z_{-L}, z_{+R}, z_{-R}, s) \\ &\quad\equiv(xx')^{q_a/2}(x'/x)^{q_b/2}Q(z_L, z_R, x) \\ &\quad=(xx')^{q_a/2}(x'/x)^{q_b/2}\sum\sigma(n_L, n_R, u)z_L{}^{n_L}z_R{}^{n_R}x^u\ , \end{aligned} \tag{2.5}$$

where u ranges over both positive and negative values. The charge constraint implicit here has been discussed by Webber.[8] Certain simple symmetry properties of Q follow immediately. If the incident charge q_a+q_b is even (odd), then n_L+n_R is even (odd), and hence

$$Q(-z_L, -z_R, x)=(-)^{q_a+q_b}Q(z_L, z_R, x)\ . \tag{2.6}$$

We will return later to this symmetry and its implications for the factorization of the generating function. Another simple property is obtained if

$$\sigma(n_L, n_R, -u)=\sigma(n_L, n_R, u)\ , \tag{2.7}$$

as would be the case, for example, in pp reactions. Consequently the generating function would then satisfy

$$Q(z_L, z_R, 1/x)=Q(z_L, z_R, x)\ . \tag{2.8}$$

In what follows we will often specialize to the case where a summation has been made over charge transfer

$$Q(z_L, z_R)=Q(z_L, z_R, 1)\ . \tag{2.9}$$

We want to now examine the consequences for the generating function (2.5) of certain general theoretical notions. In particular, we will assume that the cross sections are power bounded and that there exists an exclusive cluster decomposition in the rapidities of the produced particles.[14] When we adopt these assumptions, it becomes convenient to consider explicitly the power of s with which the generating function (2.2) grows for z_i's not unity:

$$\begin{aligned} &Q(z_{+L}, z_{-L}, z_{+R}, z_{-R}, s) \\ &\qquad\equiv\exp[p(z_{+L}, z_{-L}, z_{+R}, z_{-R}, s)Y]\ , \end{aligned} \tag{2.10a}$$

$$Y\equiv\ln(s/s_0)\ , \tag{2.10b}$$

where p will in general be a function of s. Asymptotically in s, we expect p to have a limiting value for each choice of its arguments z_i. The expansion coefficients of p for $z_{\pm L}, z_{\pm R}$ around unity, p_{ijkl}, defined in

$$\begin{aligned} p=&\sum p_{ijkl}\frac{(z_{+L}-1)^i}{i!}\frac{(z_{-L}-1)^j}{j!} \\ &\times\frac{(z_{+R}-1)^k}{k!}\frac{(z_{-R}-1)^l}{l!}\ , \end{aligned} \tag{2.11}$$

are related directly to integrals of inclusive correlation functions [recall Eqs. (2.1) and the associated discussion]. A few simple examples are as follows:

$$Yp_{1000}=\langle n_{+L}(s)\rangle=\int_{-Y/2}^{0}dy\,\rho_1(Y)\ , \tag{2.12}$$

$$\begin{aligned} Yp_{1010}&=\langle n_{+L}n_{+R}\rangle-\langle n_{+L}\rangle\langle n_{+R}\rangle \\ &=\int_{-Y/2}^{0}dy_1\int_{0}^{Y/2}dy_2C_2^{++}(y_1, y_2)\ , \end{aligned} \tag{2.13}$$

etc. Within the context of the *short-range-order* correlation picture, in which, for example, $C_2(y_1, y_2)\sim e^{-|y_1-y_2|/L}$ as $|y_1-y_2|\to\infty$, a sharp distinction exists between the coefficients p_{ijkl} which involve particles all in one hemisphere and those involving particles in both hemispheres. If the correlation functions become integrable in the rapidity differences at high energy, then it is true that for $n_L\neq0$, $n_R\neq0$ (see Ref. 7)

$$\begin{aligned} &\int_{-Y/2}^{0}dy_1\cdots dy_{n_L} \\ &\quad\times\int_{0}^{Y/2}dy_1'\cdots dy_{n_R}'\,C_{n_L+n_R}(y_1\cdots y_{n_L}; y_1'\cdots y_{n_R}') \\ &\qquad\sim\text{constant} \end{aligned} \tag{2.14}$$

as s (or equivalently Y) $\to\infty$. The implication is that whenever $i+j>1$ and $k+l>1$,

$$p_{ijkl}\to0$$

as $s\to\infty$. In contrast

$$p_{ij00}\text{ and }p_{00kl}$$

in general are nonzero, and finite as $s\to\infty$. Therefore, if the short-range-order hypothesis is correct, we can obtain a meaningful separation of p,

$$p(z_{+L}, z_{-L}, z_{+R}, z_{-R}, s) = a + p_L(z_{+L}, z_{-L}, s) + p_R(z_{+R}, z_{-R}, s) + p_c(z_{+L}, z_{-L}, z_{+R}, z_{-R}, s), \tag{2.15}$$

and we are guaranteed that $p_c \to 0$ asymptotically. Charge conservation implies further that as $s \to \infty$,

$$\exp[Yp_L(z_{+L}, z_{-L})] \sim (x'/x)^{q_b/2} \mathfrak{F}(z_L),$$
$$\exp[Yp_R(z_{+R}, z_{-R})] \sim (xx')^{q_a/2} \mathfrak{F}(z_R)$$

(read "$\mathfrak{F}$" as "function of"), and so asymptotically

$$p_L(z_{+L}, z_{-L}, s) \to p_L(z_L), \quad p_R(z_{+R}, z_{-R}, s) \to p_R(z_R). \tag{2.16}$$

The separation (2.15) can also be written, therefore, as

$$p(z_{+L}, z_{-L}, z_{+R}, z_{-R}, s) = a + p_L(z_L) + p_R(z_R) + p_c(z_L, z_R, x, x') \tag{2.15'}$$

(suppressing the s dependence), where again $p_c = O(1/Y)$ asymptotically.

To see that (2.15') is indeed what we would have expected for short-range models, but is not expected in general, we remind the reader of the energy behavior, for pp reactions, of the mean square fluctuation of the net charge transfer,

$$\langle\langle u^2 \rangle\rangle = Y \frac{\partial^2}{\partial x^2} p \Big|_{x=1}. \tag{2.17}$$

(This notation and the results below come from Ref. 6.) In models with short-range order $\langle\langle u^2 \rangle\rangle$ is expected to be constant, as implied by (2.15'), whereas in fragmentation models $\langle\langle u^2 \rangle\rangle \sim \sqrt{s}$. This can be interpreted as implying that fragmentation models have nonfactorizable singularities which will show up as strong energy dependence of moments of left-going particles as a function of right-going particles. We will discuss this point further in Sec. IV D, where data on mean squared charge transfer are presented.

To help understand the way in which (2.15') depends on the short-range-order hypothesis, a useful exercise is to compare the predictions for the two-particle correlation function $C_2(y_1, y_2)$ in short-range-order, fragmentation, and hybrid models. In the c.m. system there are four regions of interest to us: (1) quadrant I, where both particles are in the right hemisphere ($y_1 > 0$, $y_2 > 0$) [the integral over this region is $p_{02}Y$ (we are here suppressing information concerning charges)]; (2) quadrant II ($y_1 > 0$, $y_2 < 0$), whose integral is $p_{11}Y$; (3) quadrant III ($y_1 < 0$, $y_2 < 0$), whose integral is $p_{20}Y$; and (4) quadrant IV ($y_1 < 0$, $y_2 > 0$), whose integral is $p_{11}Y$ [$Y = \ln(s/s_0)$].

Short-range order. In short-range-order models, $C_2(y_1, y_2)$ depends only on $y_1 - y_2$. The maximum height of C_2 becomes constant asymptotically, with the growing part of the integral coming mainly from quadrants I and III. Ignoring energy-momentum conservation, as these effects do not change the logarithmic term, we obtain for quadrant II (or IV)

$$p_{11}Y = \tfrac{1}{2} \int_{-Y/2}^{0} dy_1 \int_{0}^{Y/2} dy_2 C_2(y_1, y_2) = \text{constant}, \tag{2.18}$$

and for quadrant I (or III)

$$p_{02}Y = \int_{-Y/2}^{0} \int_{-Y/2}^{0} dy_1 dy_2 C_2(y_1, y_2) \propto \tfrac{1}{2} Y. \tag{2.19}$$

These results coincide with (2.14), which leads to factorization of the generating function.

Fragmentation. Contrast this with the fragmentation-model[15] predictions for C_2: The only nonzero contributions to C_2 are in quadrants I and III, and the maximum height (which is at $y_1 = y_2 = 0$) increases like $\sqrt{s}$ as $s \to \infty$. The behavior in quadrants II and IV is less dramatic, and results primarily from fragmentation events created in one hemisphere yielding products which end up in the opposite hemisphere. As noted by Chou and Yang,[6] these events can account for a nonzero amount of charge transfer which grows like $\sqrt{s}$ asymptotically. If the size (area) of this region is denoted by ϵ^2, we expect

$$p_{11}Y \propto \epsilon^2 \sqrt{s}, \tag{2.20}$$

and so we predict $p_c(z_L, z_R, x)$ [Eq. (2.15')] to be extremely large asymptotically, contrary to the short-range-order prediction. In fragmentation models we definitely do not expect factorization of the generating function.

The hybrid model. A hybridization of the above two models is that there remains a *small* fraction of events in the inelastic cross section σ_{in} which are due to diffractive fragmentation, the exact fraction depending upon the energy.[16] If these events could be removed by subtraction, then the remainder would be of short-range order. The correlation function, usually defined as

$$C_2(y_1, y_2) = \frac{1}{\sigma_{in}} \frac{d^2\sigma}{dy_1 dy_2} - \frac{1}{\sigma_{in}^2} \frac{d\sigma}{dy_1} \frac{d\sigma}{dy_2}, \tag{2.21}$$

will behave differently than in short-range-order models due to σ_{in} having two components:

$$\sigma_{in} = \sigma_D + \sigma_M, \quad \sigma_D \ll \sigma_M. \tag{2.22}$$

In the central region, we assume $d\sigma_D/dy_1$, and $d^2\sigma_D/dy_1 dy_2 = 0$ so that

$$C_2(y_1, y_2) \approx \left(1 - \frac{\sigma_D}{\sigma_M}\right)\left(\frac{1}{\sigma_M}\frac{d^2\sigma_M}{dy_1 dy_2} - \frac{1}{\sigma_M^2}\frac{d\sigma_M}{dy_1}\frac{d\sigma_M}{dy_2}\right)$$

$$+ \frac{\sigma_D}{\sigma_M}\left(\frac{1}{\sigma_M^2}\frac{d\sigma_M}{dy_1}\frac{d\sigma_M}{dy_2}\right) \qquad (2.23)$$

to first order in σ_D/σ_M. For large values of $|y_1 - y_2|$, the first bracket tends to zero whereas the second bracket is constant (in the plateau region). The integrals over this plateau region then give asymptotically the results

$$p_{20}Y \propto \frac{\sigma_D}{\sigma_M}(\tfrac{1}{2}Y)^2 ,$$
$$p_{11}Y \propto \frac{\sigma_D}{\sigma_M}(\tfrac{1}{2}Y)^2 . \qquad (2.24)$$

The violation of factorization is determined by the (expected) small value of σ_D/σ_M. This can be made more reasonable by noting that this model could result from two terms, each of which factorizes:

$$\sigma(n_L, n_R) = a^D(n_L)a^D(n_R) + a^M(n_L)a^M(n_R) . \qquad (2.25)$$

The factorization property (2.15′) is therefore seen to test the form of correlation functions. What is needed to obtain factorization is the integrability of correlation functions (both exclusive and inclusive) in rapidity differences. This type of integrability is not found in all models. The resolution of whether it exists or not will ultimately come from experiment, so we now turn to the problem of experimental tests for factorization in left-right multiplicities.

B. Factorization and factorization tests

From the above results we recall that a short-range-order picture implies certain asymptotic properties (2.15′) for the generating function. These can be written in the form

$$Q(z_L, z_R, x) \sim g(z_L, z_R, x)\exp[p_L(z_L)Y] \times \exp[p_R(z_R)Y] . \qquad (2.26)$$

Specifically, this means that

$$\sigma(n_L, n_R) = \frac{1}{n_L!}\left(\frac{\partial^{n_L}}{\partial z_L^{n_L}}\right)\frac{1}{n_R!}\left(\frac{\partial^{n_R}}{\partial z_R^{n_R}}\right) Q(z_L, z_R, 1)\Big|_{z_L = z_R = 0}$$
$$\sim a_L(n_L)a_R(n_R)[1 + O(1/Y)] , \qquad (2.27)$$

the *left-right* cross section factorizes to leading order in $Y = \ln s/s_0$. This factorization property can be tested experimentally by studying the energy dependence of ratios of left-right multiplicity cross sections and comparing with the SRO prediction

$$\frac{\sigma(N, M)\sigma(K, L)}{\sigma(N, L)\sigma(K, M)} = 1 + O(1/Y) . \qquad (2.28)$$

Another set of tests of (2.26) involves the set of averages

$$\langle n_R\rangle_L \text{ vs } n_L ,$$
$$\langle n_R(n_R - 1)\rangle_L \text{ vs } n_L , \qquad (2.29)$$

etc. Some discussion of the tests (2.29) and recent NAL and CERN ISR data has been presented recently.[7] The lack of correlation expected in (2.27) implies

$$\langle n_R\rangle_L \sim cY \text{ as } Y \to \infty , \qquad (2.30)$$

where c is independent of n_L. As we will discuss in more detail in Sec. IV, the data on this test are not conclusive. In particular, the important question of whether (2.30) is true for $n_L = 1$ has not yet been answered with current data.

The energy behavior of the cross sections provides yet another test of the factorization (2.26). In particular, the following cross sections in pp collisions are related if $p_c \to 0$ in (2.15′):

$$\sigma(n_L, \text{tot}) \equiv \sum_{n_R}\sigma(n_L, n_R) \simeq (s/s_0)^{a + p_L(0) + p_R(1)} ,$$
$$\sigma(n_L, n_R) \simeq (s/s_0)^{a + p_L(0) + p_R(0)} ,$$
$$\sigma(\text{tot}) \simeq (s/s_0)^{a + p_L(1) + p_R(1)} , \qquad (2.31)$$

ignoring logarithmic factors. As an example, if the exclusive and total cross sections behave asymptotically like $(s/s_0)^{-1}$ and $(s/s_0)^0$, respectively, then $\sigma(n_L, \text{tot}) \sim (s/s_0)^{-1/2}$; i.e., the mixed quantity has an energy exponent halfway between the exclusive and inclusive quantity exponents. The vanishing of $p_c(z_L = 0, z_R = 0)$ in (2.15′) asymptotically can be tested by looking at the energy behavior of the quantities (for a general reaction now)

$$R(N, M) = \frac{\ln\sigma(N, \text{tot}) + \ln\sigma(\text{tot}, M)}{\ln\sigma(N, M) + \ln\sigma(\text{tot})} \qquad (2.32)$$

which are expected to approach $1 + O(1/Y)$ as $Y \to \infty$.

It is important to note that these tests (2.27), (2.30), and (2.32) are to be made at several energies so we can study the Y dependence of the correction terms.

At finite energy, the effect of charge conservation is to destroy the factorization expected asymptotically. In terms of the generating function for pp scattering, as an example, charge conservation imposes that the number of charges in the final state is even and greater than two. This means, for example, that the generating function has the symmetry [(2.6)]

$$Q(-z_L, -z_R) = Q(z_L, z_R) . \qquad (2.33)$$

From this it is easy to illustrate that even if the

cross sections factorize,

$$\sigma(n_L, n_R) = a(n_L)a(n_L) , \tag{2.34}$$

the generating function $Q(z_L, z_R)$ does not, except asymptotically. A particularly instructive case is

$$a(n_L) = \frac{m^{n_L}}{n_L!} , \tag{2.35}$$

which leads to the generating function

$$\begin{aligned} Q(z_L, z_R) &= \sum_{n_R + n_L \text{even}, \geq 2} \sum a(n_L)a(n_R) z_L^{n_L} z_R^{n_R} \qquad (n_L, n_R \neq 0) \\ &= \sinh(mz_L)\sinh(mz_R) \\ &\quad + \cosh(mz_L)\cosh(mz_R) - 1 \\ &= \cosh[m(z_L + z_R)] - 1 , \end{aligned} \tag{2.36}$$

which obviously satisfies the symmetry property (2.33), but does not factorize. At high energies with $m \sim c \ln(s/s_0)$, the behavior of $\ln Q(z_L, z_R)$ has the expected (factorized) form [see (2.15′)]

$$\ln Q(z_L, z_R) \sim c(z_L + z_R)Y + \text{const} + O(1/Y) . \tag{2.37}$$

C. What has to factorize

In a short-range-order picture it appears well known that the leading J-plane singularity is an isolated pole and that the above factorization constraints involving left-right multiplicities are among the consequences of the existence of this leading pole. It is important to keep in mind that several currently popular models for production processes do not possess short-range order. In particular we have seen that the hybrid diffraction-plus-multiperipheral model which has been the subject of much current theoretical speculation[16] has the feature that the correlation functions $C_n(y_1, \ldots, y_n)$ approach nonzero constants in the limit $|y_i - y_j| \to \infty$ for any pair of rapidities y_i, y_j in the central or plateau region. It is then possible for the integrated correlations in (2.14) to grow like $(\frac{1}{2}Y)^{n_L + n_R}$, both in the case that either n_L or $n_R = 0$ and for $n_L, n_R \neq 0$. There is no *a priori* reason to expect factorization from these models. It is also clear that fragmentation models need not factorize, as discussed in Sec. II A, due to the long-range correlations which can occur in them. Thus, the questions discussed here are not trivial and deserve experimental investigation. Indeed there are important theoretical reasons to believe that the leading J-plane singularity, even if it is not a simple pole, may factorize anyway. If this is true, we then have (for example) powerful restrictions on the types of hybrid models that are possible. The vanishing of $p_c(z_L, z_R, x)$, which is automatic in the short-range-order picture, may occur in complicated ways in other pictures.

One of the early results of Regge-pole theory was the observation that Regge-pole residues must factorize.[17] The impression has been gained, apparently by a sizeable segment of the physics community, that factorization is a property of poles only. In fact it has been shown by Kawai[18] that partial-wave unitarity implies that any infinity in the partial-wave amplitude must reflect certain factorization properties. Since this result bears on our investigations here, we briefly review Kawai's argument.

Suppose we have m coupled channels of scalar particles with the signatured, reduced partial-wave amplitude $B_{ij}(J, t)$ in the t channel. Time-reversal invariance makes B_{ij} symmetric,

$$B_{ij}(J, t) = B_{ji}(J, t) . \tag{2.38}$$

If the amplitude is analytic and properly bounded so the unitarity relation can be continued to complex J, we can write t-channel elastic unitarity as

$$B_{ij}(J, t) - \tilde{B}_{ij}(J, t) = 2i\rho B_{ia}(J, t)\tilde{B}_{ja}(J, t) , \tag{2.39}$$

where channel a is the elastic channel and $\tilde{B}_{ij}$ is obtained from B_{ij} by a continuation around the elastic cut. Using (2.38) and (2.39) it is easy to verify that $B_{aa}\tilde{B}_{ja} = B_{ja}\tilde{B}_{aa}$; substituting $B_{ja}\tilde{B}_{aa}/B_{aa}$ for $\tilde{B}_{ja}$ in (2.39) we obtain

$$B_{aa}(B_{ij} - \tilde{B}_{ij}) = 2i\rho B_{ia}B_{ja}\tilde{B}_{aa} . \tag{2.40}$$

If the partial-wave amplitude B_{aa} is singular,

$$\lim_{J \to \alpha} |B_{aa}(J, t)| = \infty , \tag{2.41}$$

we see that (2.39) implies

$$\lim_{J \to \alpha} \tilde{B}_{aa}(J, t) = (2i\rho)^{-1} . \tag{2.42}$$

Thus, the partial-wave amplitude B_{ij} has from (2.40) the approximate behavior as $J \to \alpha$

$$B_{ij} \simeq \frac{B_{ia}B_{ja}}{B_{aa}} ,$$

since $\tilde{B}_{ij}$ is not expected to be singular, whereas B_{ia} and B_{ja} are. It is then easy to see that the singular behavior (2.41) as $J \to \alpha$ leads to

$$B_{ij}(J, t)B_{kl}(J, t) \sim B_{ik}(J, t)B_{jl}(J, t) . \tag{2.43}$$

We thus have factorization, and are allowed to write

$$B_{ij}(J, t) = \gamma_i(t)\gamma_j(t)f(J, t) + \hat{b}_{ij}(J, t) , \tag{2.44}$$

where

$$\lim_{J \to \alpha} |f(J, t)| = \infty , \tag{2.45}$$

$$\lim_{J\to\alpha}\frac{\hat{b}_{ij}(J,t)}{f(J,t)}=0\ . \tag{2.46}$$

This factorization property depends upon unitarity and on the fact that the partial-wave amplitude is infinite at $J=\alpha$. It does not depend on this singularity being a simple pole. The most singular part of a *hard* branch point must factorize as well; a *soft* branch point such as $(J-\alpha)^{1/2}$ where the partial-wave amplitude vanishes need not factorize.

The factorization of reduced partial-wave amplitudes in coupled two-body channels does not, of course, lead directly to the factorization of left-right multiplicity distributions. It is possible to construct a chain of inference which would lead to this result, however. If (2.43) could be extended to a situation where the indices i,j ranged over quasi-two-body as well as two-body channels, we could make contact with production processes. Such an extension is plausible but has not been proved. Such a proof would require considerable theoretical effort because of technical complications involving many-particle partial-wave amplitudes such as complex helicity.[19]

If we *assume* the extension can be made and allow the indices i,j to represent the internal quantum numbers of a many-body final state, then we can obtain a constraint on production cross sections when the leading J-plane singularity obeys (2.44)–(2.46). The constraint is that the production cross section factorizes whenever any rapidity gap becomes large. That is, if we order the rapidities $y_i<y_{i+1}<y_{i+2}$,

$$d\sigma(y_1\cdots y_n)\underset{|y_i-y_{i+1}|\to\infty}{\sim}a(y_1\cdots y_i)a(y_{i+1}\cdots y_n)+O((y_i-y_{i+1})^{-\epsilon})\ . \tag{2.47}$$

This is still not sufficient to guarantee the factorization of integrated cross sections (2.28) unless the correction term is integrable in (y_i-y_{i+1}), that is,

$$\epsilon>1\ . \tag{2.48}$$

It is therefore interesting to look at differential cross sections directly and test this exclusive cluster decomposition[13] (2.47) as well as the simpler constraints on the integrated cross section (2.28).

Using the same assumption of a factorizable hard singularity in the discontinuity of a Mueller graph we can conclude that inclusive cross sections satisfy (2.47) as well as exclusive ones.

III. MODEL CALCULATIONS

Some of the underlying dynamical features of production processes which can be learned by studying left-right multiplicities will be illustrated here by means of some explicit calculations in simple models. Two pictures of hadron dynamics will be stressed: an inclusive one, as best represented by Mueller-Regge models (MRM), and an exclusive one, as best represented by multiperipheral models (MPM). It appears well known to some that the multiperipheral picture always leads to, or is expected to always lead to, an equivalent Mueller-Regge inclusive description. Recent work has taken the first step in establishing an explicit connection between these two pictures.[20] Although we believe the physics of MRM and MPM to be the same, it is nevertheless instructive to treat them separately in that certain aspects of data can be more conveniently described from one picture than the other.

A. Multiperipheral picture

The essence of the MPM can be obtained by making some crude simplifying approximations. The approximations consist of neglecting the transverse momentum dependence of the matrix element and assuming all invariant momentum transfers along the multiperipheral chain to be small so that we can reformulate the model in one (longitudinal) dimension.[10] In this reformulation, the strong-ordering limit is taken so that the only energy-momentum constraints are those fixing the total allowed interval of rapidity. If the matrix element depends only on momentum transfers, we shall call such a model the nearest-neighbor multiperipheral model (NNMM).[21] For n secondary particles produced, the differential cross section in the NNMM has the form

$$\frac{d^n\sigma}{dy_1\cdots dy_n}=g_a g_b g^n e^{(2\alpha-2)Y}f(y_1-y_a)f(y_2-y_1)\times\cdots f(y_n-y_{n-1})f(y_b-y_n)\ , \tag{3.1}$$

where g is the Reggeon-Reggeon-particle coupling squared, y_a and y_b are the initial rapidities of the beam and target ($Y=y_b-y_a$), $[e^{2\alpha y}f(y)]$ is the multiperipheral kernel, and α is the leading trajectory in the kernel. In the Chew-Pignotti model,[16] the kernel is $(s_{i,i+1}/s_0)^{2\alpha}\sim e^{2\alpha(y_{i+1}-y_i)}$, so that $f(y)=1$. The function $f(y)$ will in general not be unity due to the existence of daughter trajectories, and may be replaced by a matrix if more than one input trajectory is considered, or if isospin or charge is to be included explicitly.[22]

With the particles and rapidities labeled as in Fig. 1, the cross section for n_R particles in the region $[y_a,\ Y_R+y_a]$ and n_L particles in the region $[y_b-Y_L,\ y_b]$ (where $Y_L+Y_R=Y$) is in this approximation

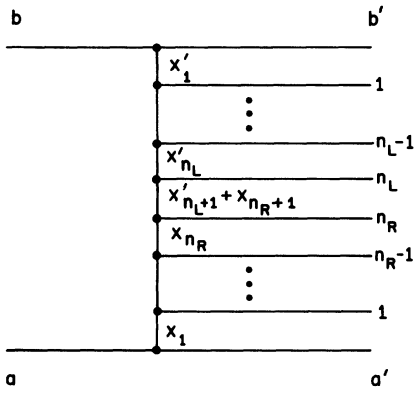

FIG. 1. The multiperipheral ladder diagram for the production process $ab\to a'b'\ n_L(\pi' s)+n_R(\pi' s)$. The phase space is assumed to be one-dimensional and the x_i shown are rapidity differences.

$$\sigma(n_L, n_R)=g_a g_b g^n e^{(2\alpha-2)Y} \times\Big|\int \prod_{i=1}^{n_L+1} dx_i'\,\delta\Big(\sum x_i' - Y_L\Big) \int \prod_{j=1}^{n_R+1} dx_j\,\delta\Big(\sum x_j - Y_R\Big) \prod_{i=1}^{n_L} f(x_i') \times \prod_{j=1}^{n_R} f(x_j) f(x'_{n_L+1}+x_{n_R+1}) \,. \quad (3.2)$$

Here x_i' and x_j are rapidity differences, and Y_L, Y_R will be treated as arbitrary. The generating function which determines the left-right multiplicities,

$$Q(z_L, z_R)=\sum_{n_L n_R} \sigma(n_L, n_R) z_L^{n_L} z_R^{n_R} \,, \quad (3.3)$$

will here refer to total rather than charged multiplicities for convenience. It is straightforward to include charge in the NNMM, but the equations become cumbersome. To evaluate (3.3), we first take a double Laplace transform of

$$Q_{n_L n_R}(Y_L, Y_R)\equiv \frac{\sigma(n_L, n_R)}{\sigma_0(Y) g^{n_L+n_R}} \qquad [\sigma_0(Y)\equiv g_a g_b e^{(2\alpha-2)Y}] \,, \quad (3.4)$$

which is defined as

$$Q_{n_L n_R}(\alpha_L, \alpha_R)\equiv \int_0^\infty dY_L e^{-\alpha_L Y_L} \times \int_0^\infty dY_R e^{-\alpha_R Y_R} Q_{n_L n_R}(Y_L, Y_R) = \bar f(\alpha_L)^{n_L} \bar f(\alpha_R)^{n_R} \frac{\bar f(\alpha_L)-\bar f(\alpha_R)}{\alpha_R-\alpha_L} \,, \quad (3.5)$$

where $\bar f(\alpha)$ is the Laplace transform of $f(y)$. Summing $Q_{n_L n_R}(z_L g)^{n_L}(z_R g)^{n_R}$ we obtain

$$Q(\alpha_L, \alpha_R)\equiv \sum Q_{n_L n_R}(z_L g)^{n_L}(z_R g)^{n_R} = \frac{1}{1-z_L g \bar f(\alpha_L)} \frac{\bar f(\alpha_L)-\bar f(\alpha_R)}{\alpha_R-\alpha_L} \times \frac{1}{1-z_R g \bar f(\alpha_R)} \,. \quad (3.6)$$

In the usual case where $f(\alpha)$ is analytic for $\mathrm{Re}\alpha>0$ and has the behavior $f(\alpha)\sim 1/\alpha$ as $\alpha\to 0$, the vanishing of $1-zg\bar f(\alpha)$ determines the leading asymptotic behavior of the inverse transform of (3.6). Denoting this solution by $p(z)$,

$$1=zgf[p(z)] \,, \quad (3.7)$$

we obtain for (3.3)

$$Q(z_L, z_R)\sim g_a g_b e^{(2\alpha-2)Y} \frac{z_L g - z_R g}{p(z_L)-p(z_R)} \frac{\rho(z_L)}{z_L g} \times e^{p(z_L)Y_L} \frac{\rho(z_R)}{z_R g} e^{p(z_R)Y_R} \,, \quad (3.8)$$

where

$$\rho(z)\equiv zp'(z)=-\frac{1}{zg\bar f'(p)} \,. \quad (3.9)$$

We note that the asymptotic behavior of σ_{in} is

$$\sigma_{\mathrm{in}}=g_a g_b e^{(2\alpha-2)Y} \frac{\rho(z)}{zg} e^{p(z)Y} \,, \quad (3.10)$$

which can be obtained directly from (3.1) or from (3.8) with $z_L=z_R=z$. The correlation between left and right depends upon the factor $(z_L-z_R)/[p(z_L)-p(z_R)]$, and we can compute explicitly the function $p_c(z_L, z_R)$ which appears in (2.15). With the constraint $p_c(z_L, 1)=0$ used in defining p_c, we obtain

$$p_c(z_L, z_R)\cong \frac{1}{Y}\left\{\ln\left[\frac{gz_L-gz_R}{p(z_L)-p(z_R)}\right]-\ln\left[\frac{g-gz_R}{p(1)-p(z_R)}\right] -\ln\left[\frac{g-gz_L}{p(1)-p(z_L)}\right]+\ln\frac{g}{\rho(1)}\right\} \,. \quad (3.11)$$

To proceed further we would need a specific model for the kernel $f(y)$. Two simple examples may serve to illustrate what can result.

The first example is the well-known Chew-Pignotti model whose kernel is $f(y)=1$ and $\alpha=\frac{1}{2}$. For this model $\bar f(\alpha)=1/\alpha$, $p(z)=zg$, and $(z_L g - z_R g)/[p(z_L)-p(z_R)]=1$. Therefore there are no left-right correlations, and $p_c(z_L, z_R)=0$.[23]

The second example is the "hard core" model of Chew and Snider.[24] In this model $f(y)=\theta(y-b)$, and $\bar f(\alpha)=e^{-\alpha b}/\alpha$. The correlation can be noted directly by computing the Laplace inverse of (3.5):

$$Q_{n_L n_R}(\alpha_L, \alpha_R) = \frac{e^{-\alpha_L n_L b}}{\alpha_L{}^{n_L}} \frac{e^{-\alpha_R n_R b}}{\alpha_R{}^{n_R}} \frac{e^{-\alpha_R b}/\alpha_R - e^{-\alpha_L b}/\alpha_L}{\alpha_L - \alpha_R} . \tag{3.12}$$

By standard techniques, we invert to obtain

$$Q_{n_L n_R}(Y_L, Y_R) = \frac{[Y_R - (n_R+1)b]^{n_R}}{n_R!} \frac{(Y_L - n_L b)^{n_L}}{n_L!} + \sum_{k=0}^{n_L} \left\{ \frac{(Y_R - n_R b)^{n_L+n_R-k}}{(n_L+n_R-k)!} \frac{[Y_L - (n_L+1)b]^k}{k!} - \frac{[Y_R - (n_R+1)b]^{n_L+n_R-k}}{(n_L+n_R-k)!} \frac{(Y_L - n_L b)^k}{k!} \right\} . \tag{3.13}$$

It can be checked that for $Y_L = Y_R = \frac{1}{2}Y$, $Q_{n_L n_R}$ is symmetric in n_L and n_R, and further that

$$\sum_{n_L+n_R} Q_{n_L n_R} = \frac{[Y-(n+1)b]^n}{n!} , \tag{3.14}$$

the result for the total multiplicity distribution in the "hard core" NNMM. There are clearly left-right correlations in (3.13) which result from the sum of components. To compute $p_c(z_L, z_R)$, we return to the asymptotic expression (3.11). The power exponent $p(z)$ is obtained by solving (3.7):

$$1 = zg \frac{e^{-p(z)b}}{p(z)} , \tag{3.15}$$

which will clearly result in a nonzero expression for $p_c(z_L, z_R)$. We leave this hard-core NNMM for the time being, since without additional input it is incapable of describing existing multiplicity data. The basic problem is that it predicts a distribution narrower than the Poisson distribution, whereas data favor a distribution (ignoring diffraction effects) slightly broader than the Poisson.

B. The KUH model

The fact that there exists a mathematical isomorphism between the multiperipheral model as formulated by DeTar[10] and the nearest-neighbor one-dimensional fluid has led to a great deal of speculation that the fluid analogy might be a way of extending our understanding of production processes.[13]

Kac, Uhlenbeck, and Hemmer[12] (KUH) have discussed in detail a one-dimensional fluid where the pair interaction consists of a hard-core repulsion (as in the Chew-Snider model) plus an exponential attraction

$$V_{\text{pair}}(y) = \gamma a e^{-\gamma y} \theta(y-b) . \tag{3.16}$$

The KUH fluid is of particular interest for hadronic processes because the corresponding generating function Q can be evaluated explicitly, and because the potential (3.16) contains a weak interaction which is not of the nearest-neighbor type or the multiperipheral type but might represent long-range interactions. There is some evidence that this type of physical mechanism does play a role in the data, and so the KUH model will be taken as an example of a model with complicated final-state interactions.

KUH show that in the limit of $\gamma \to 0$ and a fixed [i.e., $\int_0^\infty dy\, V_{\text{pair}}(y)$ fixed] the resultant energy exponent of $\sigma_{\text{tot}}(z) = s^{p(z)}$ satisfies

$$p(z) = \frac{\rho(z)}{1-\rho(z)b} - a\rho(z)^2 , \tag{3.17}$$

where $\rho(z) = zp'(z)$ as before. This equation, known as the Van der Waals equation of state, has been applied to NAL and Serpukhov multiplicity data with some success.[3(e)] Even if the KUH model were to have no physical connection to high-energy data, the formal isomorphism would still make calculations in this model instructive.

The technique which makes the interaction (3.16) soluble is an identity which reduces the calculation of the cross section involving non-nearest-neighbor interactions to that of a nearest-neighbor cross section. The price one pays is the introduction of n auxiliary integrations (for calculating σ_n). The essential point (the reader should refer to Ref. 12 for details) is that instead of (3.1), the KUH model has the form

$$\frac{d^n Q_n}{dy_1 \cdots dy_n} = \int_0^\infty dz_1 \cdots \int_{-\infty}^\infty dz_n \Psi_e(z_1) \prod_{i=1}^{n-1} [K(y_{i+1}-y_i | z_i, z_{i+1}) \theta(y_{i+1}-y_i-b)] \Psi_e(z_n) . \tag{3.18}$$

The explicit form of the kernel K in (3.18) is known, but is not important to us here. Once (3.18) is Laplace-transformed, the important quantities are the eigenvalues and eigenfunctions of the integral equation

$$\int_{-\infty}^\infty dz' K(\alpha | z, z') \Psi(z') = \lambda \Psi(z) . \tag{3.19}$$

It is known[12] that K_α is a symmetric, positive-definite Hilbert-Schmidt kernel which has a discrete set of *positive* eigenvalues $\lambda_i(\alpha)$ whose maximum is $\lambda_0(\alpha)$ and which go to zero as $i \to \infty$. The kernel therefore has a uniformly and absolutely convergent expansion in terms of its complete orthonormal set of eigenfunctions:

$$K_\alpha(z, z') = \sum_\lambda \lambda_i(\alpha)\Psi_i(z, \alpha)\Psi_i(z', \alpha) . \quad (3.20)$$

These facts allow the evaluation of $Q_n(\alpha)$:

$$Q_n(\alpha) = \sum_{i=0}^{\infty} A_i(\alpha)^2 \lambda_i{}^{n+1}(\alpha) , \quad (3.21)$$

$$A_i(\alpha) = \int_{-\infty}^{\infty} dz\, \Psi_i(z)\Psi_e(z) . \quad (3.22)$$

The calculation now proceeds as with the NNMM. The total cross section is

$$Q(\alpha) = \sum_{i=0}^{\infty} \frac{A_i(\alpha)^2 \lambda_i(\alpha)}{1 - zg\lambda_i(\alpha)} \quad (3.23)$$

and the behavior of $Q(Y)$ is determined by the leading singularities of (3.23). If the interaction (3.16) has a nonzero γ, the asymptotic behavior is determined by the vanishing of

$$1 - zg\lambda_0(\alpha) = 0 , \quad (3.24)$$

where $\lambda_0(\alpha)$ is analytic for $\mathrm{Re}\alpha > 0$ and has the behavior $e^{-\alpha b}/\alpha$ as $\alpha \to 0$. In the limit as $\gamma \to 0$, however, we have a feature not present in the simple NNMM in that an infinite number of terms in (3.23) contribute because the eigenvalues begin bunching around the function $\omega(\alpha)$, the maximum eigenvalue. It is shown in Ref. 12 that in this case $\lambda_i(\alpha) \simeq \omega(\alpha)$, and from the completeness of the eigenfunctions

$$Q(\alpha) = \frac{\omega(\alpha)}{1 - zg\omega(\alpha)} . \quad (3.25)$$

The vanishing of this denominator leads to the behavior

$$Q(Y) = \frac{\rho(z)}{zg} e^{p(z)Y} \quad (3.26)$$

for the total cross section, where $p(z)$ and $\rho(z)$ satisfy (3.17).

The steps leading to $Q(\alpha_L, \alpha_R)$ for the left-right multiplicities are analogous to those leading to (3.6), but for the subtleties involving the eigenvalues and eigenfunctions. No new complications arise which did not occur in obtaining (3.23), and so we quote the result

$$Q(\alpha_L, \alpha_R) = \sum_{i,j=0}^{\infty} \frac{A_i(\alpha_L)}{1 - z_L g\lambda_i(\alpha_L)} \frac{A_j(\alpha_R)}{1 - z_R g\lambda_i(\alpha_R)} \times \langle i, \alpha_L | j, \alpha_R \rangle \frac{\lambda_j(\alpha_R) - \lambda_i(\alpha_L)}{\alpha_L - \alpha_R} , \quad (3.27)$$

where

$$\langle i, \alpha_L | j, \alpha_R \rangle = \int_{-\infty}^{\infty} dx \Psi_i(x, \alpha_L)\Psi_j(x, \alpha_R) . \quad (3.28)$$

In the limit that $\gamma \to 0$, (3.27) simplifies due to the orthogonality of the eigenfunctions:

$$Q(\alpha_L, \alpha_R) \simeq \frac{1}{1 - z_L g\omega(\alpha_L)} \frac{\omega(\alpha_R) - \omega(\alpha_L)}{\alpha_L - \alpha_R} \times \frac{1}{1 - z_R g\omega(\alpha_R)} . \quad (3.29)$$

The result for the inverse is thus formally the same as (3.8) except now $p(z)$ satisfies a different type of equation not derivable in a MPM.

To investigate what might happen in such a model in more detail, we shall make use in Sec. IV of a simplifying approximation, known in statistical mechanics as the mean-field approximation (MFA). The approximation consists of replacing the long-range part of the non-nearest-neighbor interactions by its average value. In the KUH model, the limit $\gamma \to 0$ is meant to simulate a long-range potential. For n produced particles, the mean field approximation replaces (3.18) by

$$\frac{d^n Q_n}{dy_1 \cdots dy_n} = \prod_{i=1}^{n-1} \theta(y_{i+1} - y_i - b) e^{an^2/Y} \quad (3.30)$$

since the average potential is the number of pairs times $(1/Y)\int_0^Y dy\, V(y)$, or an^2/Y. But (3.30) is almost in the form of the Chew-Snider model, the "hard core" NNMM. The result is that the cross section $Q_{n_L n_R}(Y_L, Y_R)$ is given by (3.13) times the extra weight $e^{an^2/Y}$. In Sec. IV, this model is compared with certain aspects of the data. For completeness we give here the parameter values used, and the prescription used for including charged and neutral particles. A fit to data[3(e)] with this model favors

$$a = \tfrac{27}{64}, \quad b = \tfrac{1}{8}, \quad g = 4e^{-7/4}; \quad 2\alpha - 2 = -1 , \quad (3.31)$$

which corresponds to a Van der Waals fluid at the critical point. The distinction between neutral and charged particles is accomplished by introducing a binomial weight factor [as in Ref. 3(e)]

$$\binom{n_R}{n_R^{ch}} (\tfrac{1}{3})^{n_R - n_R^{ch}} (\tfrac{2}{3})^{n_R^{ch}}$$

for right movers, and a corresponding weight factor for left movers, into the expression (3.13). Calling $Q_{n_R n_L}$ in (3.13) $Q^{h.c.}_{n_R n_L}$, the present model is

$$\sigma_{n_R^{ch} n_L^{ch} n_R^{0} n_L^{0}} = e^{-Y} \binom{n_R^{ch}+n_R^{0}}{n_R^{ch}} (\tfrac{1}{3}g)^{n_R^{0}} (\tfrac{2}{3}g)^{n_R^{ch}} \binom{n_L^{ch}+n_L^{0}}{n_L^{ch}} (\tfrac{1}{3}g)^{n_L^{0}} (\tfrac{2}{3}g)^{n_L^{ch}} e^{an^2/Y} Q^{\text{h.c.}}_{n_L n_R}(Y_L, Y_R) , \tag{3.32}$$

with (3.31) giving the parameter values.

C. Pomeron-plus-Regge model

In applications of the types of model discussed in Secs. III A–III B, it is usually assumed that diffractive effects are small. For this reason the elastic process is excluded in these analyses. To include diffraction explicitly in the multiperipheral picture, two exchanges have to be included in the input: a Pomeranchuk pole and a secondary meson pole representing an average of all lower-lying trajectories.[16] If a matrix formalism is adopted, the formulas are similar in form to those in the NNMM of Sec. III A. In place of (3.1) we have

$$\frac{d^n\sigma_n}{dy_1 \cdots dy_n} = G_a^T F(y_1 - y_a) G F(y_2 - y_1) G \times \cdots F(y_n - y_{n-1}) G F(y_b - y_n) G_b , \tag{3.33}$$

where the kernel is now an $n \times n$ diagonal matrix if there are n poles exchanged. [We do not take out the leading behavior in the definition of F as was done in (3.1). Also we include in F the flux and phase space factor e^{-2y}.] G is an $n \times n$ matrix giving the couplings between the ith Regge pole and the jth Regge pole; G_a and G_b are column vectors of dimension n which give the coupling of the external lines to the exchanged Regge poles. Analogous to (3.5) we have the double transform of $Q_{n_L n_R}(Y_L, Y_R)$ [here $\sigma_0(Y) \equiv 1$]

$$Q_{n_L n_R}(\alpha_L, \alpha_R) = G_a^T [\overline{F}(\alpha_R) G]^{n_R} \frac{\overline{F}(\alpha_L) - \overline{F}(\alpha_R)}{\alpha_R - \alpha_L} \times [G\overline{F}(\alpha_L)]^{n_L} G_b . \tag{3.34}$$

Summing over all n_L, n_R, the analog to (3.6) is

$$Q(\alpha_L, \alpha_R) = G_a^T [I - z_L \overline{F}(\alpha_L) G]^{-1} \frac{\overline{F}(\alpha_L) - \overline{F}(\alpha_R)}{\alpha_R - \alpha_L} \times [I - z_R G \overline{F}(\alpha_R)]^{-1} G_b . \tag{3.35}$$

For comparison, we note that the Laplace transform of the total cross section is

$$Q(\alpha) = G_a^T \overline{F}(\alpha) [I - z G \overline{F}(\alpha)]^{-1} G_b . \tag{3.36}$$

We see that the leading behaviors of the cross sections are governed by the zeros of

$$\det[I - z G \overline{F}(\alpha)] = 0 . \tag{3.37}$$

In the general case, the leading behavior of the generating function $Q(Y_L, Y_R)$ will again be factorizable.

As mentioned in Sec. III A, the above formalism is general and can be used to treat the exchange of several secondary trajectories, or the effects of isospin conservation.[22] Our interest here is in the two-pole exchange model, Pomeron plus Reggeon. The treatment has to be somewhat roundabout since an input pole at $\alpha = 1$, treated in the multiperipheral formalism, is well known to generate an output pole larger than unity.[25] The difficulty remains in the inclusive picture and is connected with the vanishing of the triple-Pomeron coupling or the decoupling of the Pomeron from physical processes.[26] The standard treatment of these problems for phenomenology is to allow the Pomeron to be exchanged only once, on the argument that the Pomeron coupling is very small. For the coupling and kernel matrix we have

$$\overline{F}(\alpha) = \begin{pmatrix} 1/\alpha & 0 \\ 0 & \dfrac{1}{\alpha+1} \end{pmatrix}, \quad G = \begin{pmatrix} 0 & \gamma \\ \gamma & g \end{pmatrix} , \tag{3.38}$$

assuming the Pomeron to be at 1 and the secondary exchange to be at $\frac{1}{2}$. These intercepts are taken to be only approximations and might be varied. For calculating multiplicities, the relevant quantity is

$$[\overline{F}(\alpha)G]^n \cong \begin{pmatrix} \delta_{n0} & \dfrac{\gamma}{\alpha}\left(\dfrac{g}{\alpha+1}\right)^{n-1}\theta(n-1) \\ \dfrac{\gamma}{\alpha+1}\left(\dfrac{g}{\alpha+1}\right)^{n-1}\theta(n-1) & \dfrac{g}{\alpha+1}\left(\dfrac{g}{\alpha+1}\right)^{n-1} \end{pmatrix} . \tag{3.39}$$

After some algebra, and neglecting terms of order γ^2 and higher, we find that (3.34) has the form

$$Q_{n_L n_R}(\alpha_L, \alpha_R) = \gamma_e^a \gamma_e^b \frac{\delta_{n_L 0}}{\alpha_L} \frac{\delta_{n_R 0}}{\alpha_R} + g_a g_b \frac{g^{n_L+n_R}}{(\alpha_L+1)^{n_L}(\alpha_R+1)^{n_R}}$$
$$+\gamma_e^b g_a \left(\frac{\delta_{n_L 0}}{\alpha_L} \frac{\gamma g^{n_R-1}\theta(n_R-1)}{\alpha_R(\alpha_R+1)^{n_R}} + \frac{\gamma g^{n_L-1}\theta(n_L-1)}{\alpha_L(\alpha_L+1)^{n_L}} \frac{g^{n_R}}{(\alpha_R+1)^{n_R+1}} \right)$$
$$+\gamma_e^a g_b \left(\frac{\delta_{n_R 0}}{\alpha_R} \frac{\gamma g^{n_L-1}\theta(n_L-1)}{\alpha_L(\alpha_L+1)^{n_L}} + \frac{\gamma g^{n_R-1}\theta(n_R-1)}{\alpha_R(\alpha_R+1)^{n_R}} \frac{g^{n_L}}{(\alpha_L+1)^{n_L+1}} \right) . \quad (3.40)$$

The significance of these terms and a comparison of this type of model with data has been done by Snider.[27] We summarize briefly the physics of (3.40). The first two terms are the elastic scattering given by Pomeron exchange ($\gamma_e^a \gamma_e^b$) and the multiperipheral contribution to $\sigma(n_L, n_R)(g_a g_b)$. The latter is here given by the product of two Poisson distributions. The last two terms represent low- and high-mass diffraction. For example the terms proportional to $\gamma_e^b g_a$ consist of (1) Pomeron exchange extending across the left hemisphere to a low-mass state in the right hemisphere—low-mass diffraction; and (2) Pomeron exchange which remains in the left hemisphere to a high-mass state—high-mass diffraction. We note that the inverse transform of these diffraction parts,

$$\frac{1}{2\pi i} \int_{c-i\infty}^{c+i\infty} d\alpha [e^{\alpha Y}] \frac{\gamma g^{n-1}\theta(n-1)}{\alpha(\alpha+1)^n} = \gamma g^{n-1} \left[1 - e^{-Y} \sum_{k=0}^{n-1} \frac{Y^k}{k!} \right] , \quad (3.41)$$

which is an incomplete gamma function, has been discussed previously with regard to multiplicity data.[28]

The factorization properties of (3.40) are most easily seen by writing the equation in the form

$$Q_{n_L n_R}(\alpha_L, \alpha_R) = A^a_{n_R}(\alpha_R) A^b_{n_L}(\alpha_L) + B^a_{n_R}(\alpha_R) B^b_{n_L}(\alpha_L) , \quad (3.42a)$$

$$A^i_n(\alpha) = \gamma_e^i \frac{\delta_{n0}}{\alpha} + g_i \gamma \frac{g^{n-1}\theta(n-1)}{\alpha(\alpha+1)^n} , \quad (3.42b)$$

$$B^i_n(\alpha) = \frac{g_i g^n}{(\alpha+1)^{n+1}} + \frac{\gamma_e^i \gamma g^{n-1}\theta(n-1)}{\alpha(\alpha+1)^n} . \quad (3.42c)$$

Both terms in (3.42a) give leading behavior in the approximation that $(\gamma Y)^2$ is negligible, and so the generating function $Q(z_L, z_R)$, which will have the form

$$Q(z_L, z_R) = A^a(z_R) A^b(z_L) + B^a(z_R) B^b(z_L) , \quad (3.43)$$

will not factorize. This lack of consistency with the starting assumptions is clearly related to our being forced for other reasons to keep only one Pomeron exchange in the approximation. To compare the basic features of this picture with data we simplify (3.40) somewhat while retaining the basic form (3.42). This will be explained in more detail in Sec. IV.

D. Inclusive picture

It is interesting to counterbalance the above microscopic, or exclusive, models for left-right multiplicities with a simple Mueller-Regge model for the inclusive multiplicity moments $f_{n_L n_R}$. We choose for this purpose the model of Frazer, Peccei, Pinsky, and Tan (FPPT).[3(f)] It is assumed that the inclusive correlation functions are dominated by their values in the central region, and further that these values can be well approximated by the Regge form even down to small rapidity differences. The diagrams considered are shown in Fig. 2. Formally the contributions of Fig. 2 have the MPM form (3.33) for Q_n and (3.34) for $Q_{n_L n_R}$ with G and F 2×2 matrices,

$$G = \begin{pmatrix} g_{PP} & g_{PM} \\ g_{PM} & g_{MM} \end{pmatrix} , \quad \bar{F}(\alpha) = \begin{pmatrix} 1/\alpha & 0 \\ 0 & \frac{1}{\alpha+\frac{1}{2}} \end{pmatrix} , \quad (3.44)$$

and the external couplings two-dimensional column vectors,

$$G_a = G_b = \begin{pmatrix} 1 \\ 0 \end{pmatrix} . \quad (3.45)$$

We assume the meson trajectory is at $\alpha = \frac{1}{2}$, the Pomeron is $\alpha = 1$, and the particles are in the cen-

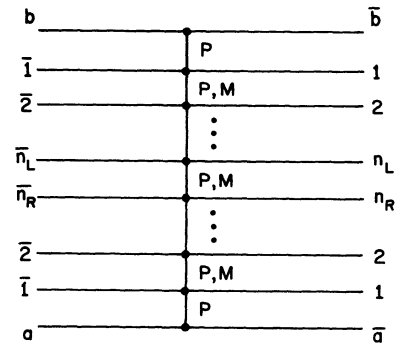

FIG. 2. The multiperipheral Mueller diagram which contributes to the $(n_L + n_R)$-particle inclusive correlation function.

tral region so that the external meson coupling can be ignored. To compute the integrated correlation functions f_n, we use the identities

$$\sum_{n=0}^{\infty} Q_n (z-1)^n = \exp\left[\sum_{n=1}^{\infty} f_n \frac{(z-1)^n}{n!}\right] , \tag{3.46}$$

$$\sum_{n_L, n_R=0}^{\infty} Q_{n_L n_R} (z_L - 1)^{n_L} (z_R - 1)^{n_R}$$

$$= \exp\left[\sum_{n_L, n_R=1}^{\infty} f_{n_L n_R} \frac{(z_L-1)^{n_L}}{n_L!} \frac{(z_R-1)^{n_R}}{n_R!}\right] \tag{3.47}$$

so that the results for $Q(\alpha_L, \alpha_R)$, $Q(\alpha)$, and $\det[I - zG\bar{F}(\alpha)] = 0$ are the same as (3.35)–(3.37) with all z's replaced by $z-1$. The zeros of $\det[I-(z-1)G\bar{F}(\alpha)]$,

$$\frac{1}{\alpha(\alpha+\frac{1}{2})}\{[\alpha-(z-1)g_{PP}][\alpha+\tfrac{1}{2}-(z-1)g_{MM}] - (z-1)^2 g_{PM}^2\} = 0 , \tag{3.48}$$

determine the leading behavior of the generating function $Q(\alpha)$ and $Q(\alpha_L, \alpha_R)$. For $Q(Y)$ the result is

$$Q(Y) \simeq \frac{p_+(z) + \frac{1}{2} - (z-1)g_{MM}}{p_+(z) - p_-(z)} \exp[p_+(z)Y] , \tag{3.49}$$

where[29]

$$p_\pm(z) = \tfrac{1}{2}[-\tfrac{1}{2} + (z-1)(g_{MM}+g_{PP})] \pm \tfrac{1}{2}\{[\tfrac{1}{2} + (z-1)(g_{PP}-g_{MM})]^2 + 4(z-1)^2 g_{PM}^2\}^{1/2} \tag{3.50}$$

are the solutions for (3.48). The result for $Q(z_L, z_R)$ is

$$Q(z_L, z_R) \cong \frac{[p_+(z_L) + \frac{1}{2} - (z_L-1)g_{MM}][p_+(z_R) + \frac{1}{2} - (z_R-1)g_{MM}] + (z_L-1)(z_R-1)g_{PM}^2}{[p_+(z_L) - p_-(z_L)][p_+(z_R) - p_-(z_R)]} \exp[p_+(z_L)Y_L + p_+(z_R)Y_R] . \tag{3.51}$$

We see now explicitly that the left-right correlations $p_c(z_L, z_R)$ go to zero like $1/Y$ as $Y \to \infty$, which further illustrates the points made in Sec. II. Additionally we see the formalism of the Mueller-Regge picture closely parallels that of the MPM, justifying our including them in the same general picture. Finally, we note that it is a simple generalization to include isospin constraints explicitly in the above formalism. The coupling and kernel matrices then have a larger dimension.

IV. IMPLICATIONS FOR THE DATA

With the continuing analysis of bubble chamber[30] and two-arm spectrometer[31] data on high-energy pp collisions, we are beginning to obtain the experimental values for the left-right charged cross sections $\sigma(n_L, n_R)$, the average multiplicities $\langle n_L \rangle$ vs n_R, the mean-squared charge transfer $\langle u^2 \rangle$, and the other coarse-grained quantities we have been discussing. The currently available amount of data on these quantities is not large, and there is still a lot of important information which can be obtained from analyses of experiments *below* NAL energies. For example, the question of the energy dependence of the experimental quantities $R(N, M)$ in Eq. (2.32) requires measurements of left-right multiplicities in the AGS-ZGS energy range.

One thing which can be done with the data currently available is to examine the problem of separating that portion of the inelastic cross section which might be labeled diffractive fragmentation in a hybrid or two-component theory. This problem is important because it strikes at the viability of the two-component concept. If the diffractive and short-range components cannot be separated, then it is not clear whether we can attach much significance to the two-component models currently being discussed.

A. The two-component concept and $\sigma(n_L, \text{tot})$

The idea that a certain fraction of inelastic events in asymptotic proton-proton collisions contain a quasielastically scattered proton in one hemisphere and an excited "fireball" which decays into two or more particles in the other hemisphere has received a good deal of attention.[15] Only recently has it become apparent that these types of events do not dominate production processes at current energies.[9] The experimental observation of a low-mass enhancement in the inclusive cross section $pp \to p + \text{MM}$ at NAL and ISR,[32] however, provides sufficient evidence that there are some of these events.

Currently, the most frequently discussed possibility is a hybrid model for production processes containing both a fragmentation component and a short-range-order component. There remain several important unanswered questions in the two-component approach, such as whether the dominant excitation of the "fireball" at current energies is due to Pomeron exchange. These questions can only be answered cleanly if there is some way of looking at the data which separates the two components so that each can be discussed separately.

In some versions of the two-component model, the charged-prong multiplicity distribution would, at infinite energy, develop a dip structure, the diffractive component contributing only to low multiplicity. If this characteristic were present in the data, it would be possible to make the separation into two components comparatively easily. The dip structure is certainly not present in the data at NAL energies, and so a separation on the basis of total charged multiplicities is not possible. In addition there is a certain theoretical uncertainty about whether any dip in the multiplicity distribution is really expected. A "self-consistent" model due to Ball and Zachariasen,[28] for example, has several features in common with the other versions of the two-component approach, except the "diffractive" component contributes to cross sections out to the mean multiplicity. In this version of the two-component model no dip would develop, but only a broad plateau. A related approach due to Frazer, Snider, and Tan[16] also predicts no dip.

We have to look at slightly more complicated objects than the total charged-prong distribution in order to isolate the diffractive component. Since the Pomeron has isospin zero, it will contribute asymptotically only to those cross sections where the charge transfer between hemispheres is zero. In proton-proton collisions, this means for example that the total charge in the forward hemisphere due to a diffractive event must be +1. If we look at the distribution $\sigma(n_L, \text{tot})$ vs n_L, then diffractive processes will contribute only to those cross sections with n_L odd. It is not hard to convince oneself that the most plausible situation is for a substantial portion of the diffractive cross section to be in $\sigma(1, \text{tot})$. This is the cross section which contains those events in which there is a quasielastic proton in the left hemisphere. By symmetry, there are an equal number of events containing a quasielastic proton in the right hemisphere. In the plot of $\sigma(n_L, \text{tot})$ these show up in $\sigma(1, \text{tot})$, $\sigma(3, \text{tot})$, $\sigma(5, \text{tot})$, etc. The graph in Fig. 3 shows preliminary experimental data on $\sigma(n_L, \text{tot})$ at $p_{\text{lab}} = 205$ GeV/c.[30] The theoretical curves represent parametrizations based on models discussed in Sec. III and are explained more fully in the figure caption. The data completely support the qualitative expectations of the two-component picture. The presence of the expected large surplus of events in $\sigma(1, \text{tot})$ followed by a dip in $\sigma(2, \text{tot})$ is reinforced by the sawtooth behavior of the rest of the distribution showing the tendency to prefer odd multiplicities (and, presumably, $\Delta Q = 0$) over even multiplicities. The presence of the dip allows us to extrapolate roughly the nondiffractive component and estimate

$$\sigma(1, \text{tot})_{\text{diff}} \cong 3.5 \text{ mb}. \tag{4.1}$$

It might be noted parenthetically that this distribution is the first *inelastic* multiplicity distribution to show any sort of dip structure.

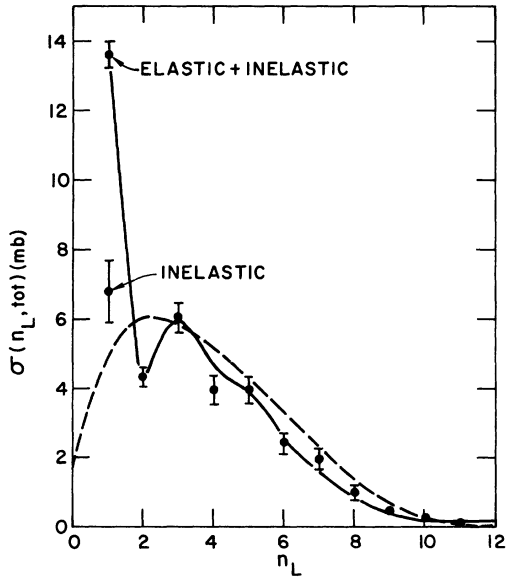

FIG. 3. Preliminary experimental data on $\sigma(n_L, \text{tot})$ from the ANL-NAL collaboration at $p_{\text{lab}} = 205$ GeV/c (Ref. 30). The two theoretical curves are motivated from models discussed in Sec. III. The dashed curve is the prediction of a critical-point fluid model given by Eq. (3.32) with the parameters (3.31). The smooth curve is a two-component model with

$$\sigma(n_L, n_R) \propto \left(\frac{1}{n_L^2} \frac{1}{n_R^2} + 4.8 \frac{e^{-4}(4)^{n_L}}{n_L!} \frac{e^{-4}(4)^{n_R}}{n_R!} \right).$$

This parametrization retains the basic features of (3.43).

B. Estimates of the diffractive component from $\sigma(n_L, n_R)$

To get more information about the amount of fragmentation or diffraction we can look at the distribution of $\sigma(n_L, n_R)$ directly. As pointed out by Nussinov, Quigg, and Wang,[5] it is possible to distinguish between the extremes of pure fragmentation models and pure short-range-order models in a single experiment at a fixed energy by looking at the shape of $\sigma(n_L, N - n_L)$ as a function of n_L. It is easy to see how this can be if we assume exact factorization,

$$\sigma(n_L, N - n_L) = a(n_L) a(N - n_L) . \tag{4.2}$$

Recall now that the short-range-order concept discussed in Sec. II would require that both $a(n_L)$ and $a(N - n_L)$ be peaked around some central value $\langle n \rangle \propto \ln s$ and that they fall off rapidly for values of n larger or smaller than $\langle n \rangle$. We can see that in a

short-range-order picture $\sigma(n_L, N-n_L)$ will be maximum near the symmetric distribution $n_L = N-n_L$. The most popular "fragmentation" models would favor either n_L or $N-n_L$ small, so that the antisymmetric distribution is preferred. The specific examples of $a(n_L)$ being Poisson or $1/n_L^2$ are discussed by Nussinov, Quigg, and Wang.

The general feature of short-range order contributing mainly near $\langle n_L \rangle$ and "fragmentation" or "diffraction" contributing to small n_L should be true as well in two-component models, so looking at $\sigma(n_L, N-n_L)$ should aid in the *separation* of fragmentation and short-range order. Preliminary data at 205 GeV/c are shown in Fig. 4 compared with a critical-point fluid model and a two-component model based on the discussion in Sec. III. A model-independent statement can also be made. Except for the four-prong events, the data favor the symmetric distribution of left-right multiplicities implied by the short-range-order concept. The apparent surplus of events in $\sigma(3,1)$ can be understood if the "fragmentation" component is entirely "diffractive" in that $I=0$ Pomeron exchange dominates. In the same experiment a more detailed analysis of the four-prong events has been performed. Figure 5 shows the missing mass

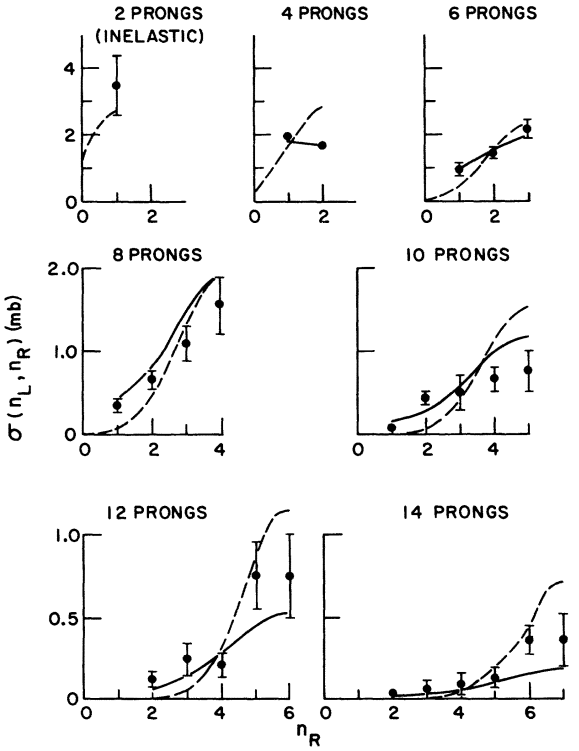

FIG. 4. Data on $\sigma(n_L, n_R)$ at 205 GeV/c from the ANL-NAL collaboration (Ref. 30) presented at fixed prong number $N = n_L + n_R$ as a function of n_L. The theoretical curves are from the same models as in Fig. 3.

spectrum of $pp \to pX$ in the different four-prong charge configurations.[32] Not surprisingly, we see a low-mass enhancement in $\sigma(1, 3)$ not present in either $\sigma(2, 2)$ or $\sigma(3, 1)$. If we identify the experimental cross section for producing this enhancement,

$$\sigma_D(1, 3) = 0.82 \pm 0.07 \text{ mb}, \tag{4.3}$$

with the diffractive component we then conclude that the diffraction and short-range-order components in $\sigma(1, 3)$ are about equal at this energy.

Snider[27] has done an analysis of the same data based on an assumption of a factorizable Pomeron. He obtains a larger diffractive component,

$$\sigma_D(1, 3) = 1.35 \text{ mb}, \tag{4.4}$$

than the experimental low-mass enhancement. In his approach, however, it is quite reasonable to expect a large component of diffraction in the high missing mass as well as a diffractive component in $pp \to (n\pi^+)X$ which are difficult to separate from the short-range order.

Equations (4.1) and (4.3) are consistent if we assume that $\sigma(1,1)$ is predominantly diffractive and that the amount of diffraction in $\sigma(1, 5)$, etc. is small.

The obvious test for the presence of diffraction is, of course, the energy dependence of the cross sections. Figure 6 shows what data there are on the energy dependence of the four-prong data. In this plot $\sigma(1, 3)$ is compared with $\sigma(0, 4) + \sigma(2, 2)$.

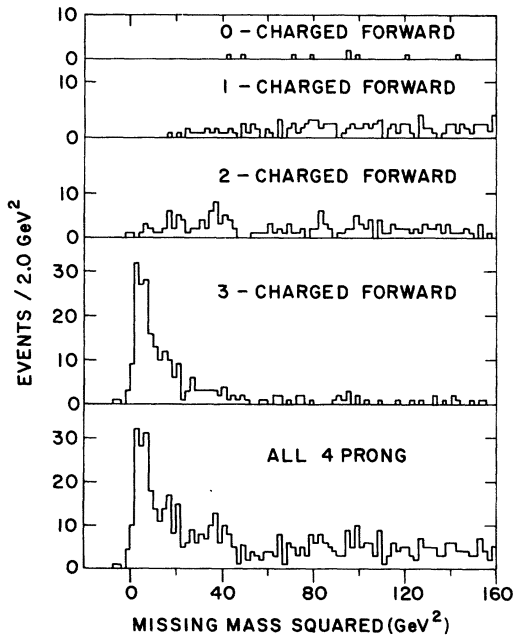

FIG. 5. The missing-mass spectrum off the slow proton in the four-prong events at 205 GeV/c for different left-right charge configurations (Ref. 32).

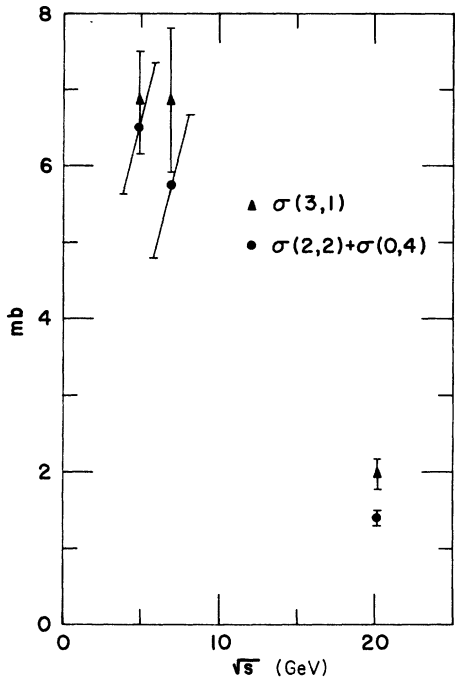

FIG. 6. The energy dependence of the cross sections $\sigma(1,3)=\sigma_{\Delta Q=0}$ and $\sigma(0,4)+\sigma(2,2)=\sigma_{\Delta Q=1}$ as a function of energy. The data at 12 and 24 GeV/c are from the Bonn-Hamburg-München collaboration. The 205-GeV/c data are from the ANL-NAL collaboration (Ref. 30).

Since Pomeron exchange should not contribute asymptotically to $\Delta Q=1$ the latter cross section should be free of diffraction. The experimental errors are certainly large, but there is not much indication for a different dependence. The energy dependence alone is consistent with the diffractive component in $\sigma(1,3)$ being zero, but it can be as large as that given by (4.3).

A related test for the presence of diffraction involves plotting the data as a function of the maximum rapidity gap in the event and the charge transferred across that gap. Data on this are available at $p_{\text{lab}}=12$ and 24 GeV. Since this quantity can in principle separate diffractive events with large missing mass, data at higher energies would provide a check on the considerations presented here.

C. Average multiplicities and factorization

As indicated in the discussion of Sec. III C concerning the two-pole–nearest-neighbor–multiperipheral model, the standard formulation of the hybrid or two-component model is explicitly not factorizable in left-right multiplicities. We can define the hybrid model by writing the total cross section in the form

$$\sigma_{\text{tot}}=\sigma^D+\sigma^S\,, \tag{4.5}$$

where σ^D is a diffractive piece and σ^S a short-range-order piece. A large fraction of the elastic cross section is usually grouped with the diffractive portion. The arguments presented in Sec. II B concerning the short-range-order component indicate that it separately should asymptotically factorize with respect to left-right multiplicities. If the Pomeranchuk singularity is a hard one, as discussed in Sec. II C, then the diffractive piece associated with single Pomeranchuk exchange should also factorize. At high energy, it may therefore make sense to write

$$\sigma(n_L,n_R)\cong a^D(n_L)a^D(n_R)+a^S(n_L)a^S(n_R)\,, \tag{4.6}$$

where we have to keep track of the fact that the diffractive piece contributes only to those distributions where no charge is exchanged between left and right hemispheres. In terms of the two-pole–nearest-neighbor–multiperipheral model discussed in Sec. III, it is interesting to note that we recover the factorization properties (4.6) if we group "high-mass diffraction" with the short-range component.

The consequences of the factorization properties of (4.6) are most clearly seen in the energy dependence of the quantities

$$\langle n_L\rangle_{n_R}\cong\frac{\sum_{n_L}n_L[a^D(n_L)a^D(n_R)+a^S(n_L)a^S(n_R)]}{\sum_{n_L}[a^D(n_L)a^D(n_R)+a^S(n_L)a^S(n_R)]}\,, \tag{4.7}$$

with the usual assumption that at high energy $a^S(n_R)$ is peaked at $\langle n_R\rangle\approx\ln s$ while $a^D(n_R)$ is energy-independent and peaked at small n_R ($n_R=1$ in pp collisions). We therefore get

$$\langle n_L\rangle_{n_R=1}\cong\frac{\sum_{n_L}n_La^D(n_L)}{\sum_{n_L}a^D(n_L)}\to\text{const.} \tag{4.8}$$

For charge configurations in which diffraction cannot contribute, such as $n_R=2$ in pp collisions, which must have charge transfer, or for right multiplicities large we obtain

$$\langle n_L\rangle_{n_R=2}\cong\langle n_L\rangle_{n_R\approx\langle n_R\rangle}$$

$$\cong\frac{\sum n_La^S(n_L)}{\sum a^S(n_L)}\propto\ln s\,. \tag{4.9}$$

There is some evidence for this distinction between $\langle n_L\rangle_{n_R=1}$ and other values of n_R in the ANL-NAL data[30] at 205 GeV/c. The fact that data from ISR do not show this distinction can perhaps be understood from the fact that the spectrometers in the ISR experiment do not detect events in a cone of about 4° around the forward direction. They therefore miss most of the diffractive events and are insensitive to the possibility of two production mechanisms. Data from the NAL experiment are shown in Fig. 7. The theoretical curves are again the

fluid model and a version of the hybrid model.

Note that if we write asymptotically an explicitly factorized form for $\sigma(n_L, n_R)$,

$$\sigma(n_L, n_R) \cong [\gamma b^D(n_L) + b^S(n_L)]\,[\gamma b^D(n_R) + b^S(n_R)]\ , \tag{4.10}$$

we can still incorporate the idea of two types of production mechanisms. It is not easy to disentangle the various terms of this kind of *ad hoc* factorizing hybrid model to each $\sigma(n_L, n_R)$. If we neglect terms of $O(\gamma^2)$, the structure is quite similar to the usual hybrid model. In the factorized form we have explicitly the result

$$\langle n_L \rangle_{n_R=1} \simeq \langle n_L \rangle \propto \ln s\ . \tag{4.11}$$

Since many current approaches to the two-component model present it as consisting of the first two terms in a power-series expansion in something like $g_{PPP}\ln s$, where g_{PPP} is a triple-Pomeron coupling, it is perhaps premature to rule out the possibility that at superasymptotic energies we recover factorization in left-right multiplicities. It is not clear, therefore, that the prediction (4.8) is an absolute test of these ideas. However, it is clear that measurements of $\langle n_L \rangle_{n_R}$ at several energies through the ASG-ISR range can supply a great deal of information with little fuss.

The factorization test (2.28) can also be used to investigate the possibility of a two-component structure such as (4.6). Keeping in mind the fact that $a^D(n_L)$ will only contribute to odd $n\,(u=0)$, we would predict that ratios of cross sections involving only even multiplicities would be much closer to unity than those involving odd multiplicities. In the 205-GeV/c data we have, for example,

$$\frac{\sigma(2,2)\sigma(4,4)}{\sigma(2,4)\sigma(2,4)} = 1.3 \pm 0.3\ , \tag{4.12}$$

$$\frac{\sigma(3,3)\sigma(5,5)}{\sigma(3,5)\sigma(3,5)} = 1.8 \pm 0.6\ . \tag{4.13}$$

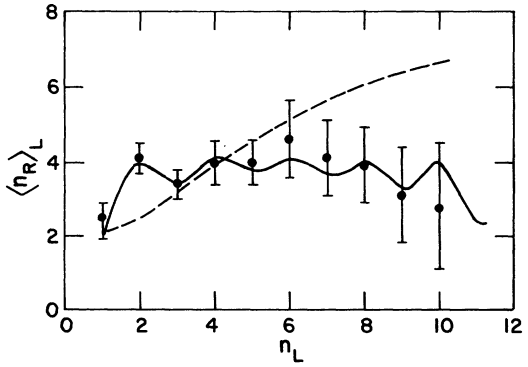

FIG. 7. Data on $\langle n_L \rangle_{n_R}$ from the 205-GeV/c bubble chamber experiment at NAL (Ref. 30).

If this tendency is observed at other energies it will be an important confirmation of these ideas.

D. Data on charge transfer

The energy behavior of the mean-squared charge transfer between hemispheres has been proposed as a feature of the data which will distinguish short-range-order and fragmentation models.[6] We define the charge transfer

$$\langle\langle u^2 \rangle\rangle = \sigma_{\text{tot}}^{-1} \sum_{n_L, n_R, u} u^2 \sigma(n_L, n_R, u)\ . \tag{4.14}$$

In models with short-range order it is well known that

$$\langle\langle u^2 \rangle\rangle_{\text{SRO}} \sim \text{const}\ . \tag{4.15}$$

The simple arguments given in Sec. II in terms of the generating-functional formalism confirm this result. See, for example, Eqs. (2.15′) and (2.17).

The arguments for the behavior of $\langle\langle u^2 \rangle\rangle$ in the diffractive fragmentation picture are slightly more complicated. In these models we have for large s

$$\sigma(n_L, n_L, u) \to 0, \quad u \neq 0 \tag{4.16}$$

but the summation over n_L, n_R in (4.14) diverges at large n to give

$$\langle\langle u^2 \rangle\rangle_{\text{Chou-Yang}} \propto s^{1/2}\ . \tag{4.17}$$

This is another example of the general feature of diffractive fragmentation models of large correlations in the central region from high-multiplicity events. The hybrid model in this case does not predict a behavior for the charge transfer intermediate between the short-range-order and frag-

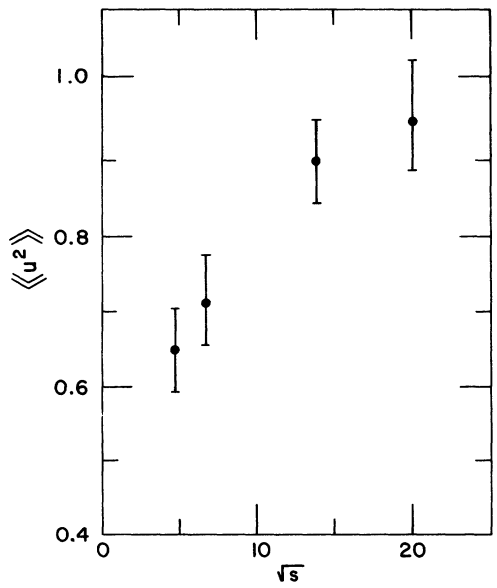

FIG. 8. Data on $\langle\langle u^2 \rangle\rangle$ vs $\sqrt{s}$ (Ref. 30).

mentation pictures. To see this we write

$$\sigma(n_L, n_R, u) = \sigma^D(n_L, n_R, u) + \sigma^S(n_L, n_R, u) \quad (4.18)$$

and input the usual assumptions about the diffractive component:

$$\sigma^D(n_L, n_R, u) \to 0, \quad u \neq 0 \quad (4.19)$$

$$\sigma^D(n_L, n_R, u) = 0, \quad n_L + n_R > N \quad (4.20)$$

where N is some (approximate) energy-independent integer. In the hybrid picture no energy-dependent divergence of the sum (4.14) takes place and

$$\langle\langle u^2 \rangle\rangle_H \sim \sigma_{\text{tot}}^{-1} \sum_{n_L, n_R, u} u^2 \sigma^S(n_L, n_R, u) \sim \text{const} ; \quad (4.21)$$

the mean squared charge transfer behaves asymptotically just as it does in a short-range-order model.

The available data on charge transfer is shown in Fig. 8. The fact that we see little experimental evidence for the approach to a constant asymptotically indicates that the correction terms to factorization of the generating function $p_c(z_L, z_R, s)$ discussed in Sec. II may be large at available energies. This does not mean that the ideas presented in Sec. II should not be investigated experimentally. The suggestion is that the correction terms are large, and this means that the energy dependence of quantities such as $R(N, M)$ in Eq. (2.32) will provide nontrivial information.

V. SUMMARY AND CONCLUSIONS

The analysis of data on hadronic production processes is becoming more sophisticated, as some of the simple early questions have been answered. We are still at a primitive stage in our understanding, however, so it is important to be flexible in our approach. In this paper we have considered what can be learned from left-right multiplicities. Data on left-right multiplicities are easy to obtain and can provide important dynamical information both at intermediate and high energies. Along with other coarse-grained or integrated quantities, left-right multiplicities illustrate the advantages of dealing with exclusive and inclusive data on an equivalent footing.

As an example of the dynamic questions which left-right multiplicities can provide we have seen how the short-range order concept leads to factorization. This left-right factorization can be interpreted as a consequence of the presence of a leading Regge pole in the short-range-order framework. Left-right factorization is not a universal property of models for the production process, but, due to the fact that unitarity[18] and other constraints[33] favor approximately factorizable J-plane singularities, we discuss a series of tests for this property. Data at low energies are needed so that we can see if there is an approach to factorization. The indication from the behavior of charge transfer is that correction terms may be large.

Another feature of left-right multiplicities is that they are sensitive to the presence of a diffractive component in the production mechanism. Preliminary data at 205 GeV/c give a good measure of the amount of diffraction in $\sigma(1, 3)$ and $\sigma(1, \text{tot})$.

ACKNOWLEDGMENTS

We are grateful for early conversations with Lloyd Hyman and Rich Singer concerning the ANL-NAL data which stimulated our interest in this project. We thank Carl Bromberg and Tom Ferbel for sending us a preliminary analysis of the 102-GeV/c data and Brian Musgrave for providing us with $pp \to pX$ missing-mass data at 205 GeV/c. For many important conversations, we are indebted to R. Arnold and Dale Snider.

---

*Work performed under the auspices of the U. S. Atomic Energy Commission.

[1]Charged-particle multiplicity distributions from NAL can be found as follows for pp reactions. 103 GeV/c: J. W. Chapman *et al.*, Phys. Rev. Lett. 29, 1686 (1972). 205 GeV/c: G. Charlton *et al.*, *ibid.* 29, 515 (1972). 303 GeV/c: F. T. Dao *et al.*, *ibid.* 29, 1627 (1972). For πp multiplicities at NAL, 205 GeV/c: D. Bogert *et al.*, Phys. Rev. Lett. 31, 1271 (1973). Preliminary multiplicity distributions at the ISR can be found in *Proceedings of the XVI International Conference on High Energy Physics, Chicago-Batavia, Ill., 1972*, edited by J. D. Jackson and A. Roberts (NAL, Batavia, Ill., 1973); see in particular G. Bellettini, Vol. 1, p. 279, and J. Whitmore, Vol. 1, p. 224. 50-, 69-GeV/c pp reactions at Serpukhov: V. V. Ammosov *et al.*, Phys. Lett. 42B, 519 (1972). 33.8-GeV/c K^-p and 50-GeV/c π^-p reactions at Serpukhov: V. V. Ammosov *et al.*, Nucl. Phys. B58, 77 (1973).

[2]One- and two-particle inclusive distributions at ISR can be found in G. Bellettini's talk (Ref. 1) as well as in M. Jacob's review, in *Proceedings of the XVI International Conference on High Energy Physics, Chicago-Batavia, Ill., 1972* (Ref. 1), Vol. 1, p. 373. Inclusive distributions at NAL can be found in the review talk by J. Whitmore, in *Experiments on High Energy Particle Collisions—1973*, proceedings of the international conference on new results from experiments on high energy particle collisions, Vanderbilt University, 1973, edited by Robert S. Panvini (A.I.P.,

New York, 1973), p. 14; see also Y. Cho *et al.*, Phys. Rev. Lett. 31, 413 (1973).

[3]We list a representative sample of proposed models for multiplicity distributions.

(a) Independent-emission models: D. Sivers and G. H. Thomas, Phys. Rev. D 6, 1961 (1972); G. H. Thomas, *ibid.* 7, 2058 (1973).

(b) Nova model: E. L. Berger, Phys. Rev. Lett. 29, 887 (1972).

(c) "KNO" scaling models: Z. Koba, H. B. Nielsen, and P. Olesen, Nucl. Phys. B40, 317 (1972); P. Olesen, Phys. Lett. 41B, 602 (1972); P. Slattery, Phys. Rev. Lett. 29, 1627 (1972).

(d) "Two-component models": J. D. Jackson and C. Quigg, NAL report, 1972 (unpublished).

(e) Bjorken-Feynman-Wilson fluid analog: R. C. Arnold and G. H. Thomas, Phys. Lett. (to be published); G. H. Thomas, Phys. Rev. D 8, 3042 (1973).

(f) Mueller-Regge models; W. R. Frazer, R. D. Peccei, S. S. Pinsky, and C.-I Tan, Phys. Rev. D 7, 2647 (1973). These authors consider also a two-component model, and give further references concerning such models.

[4]A. Mueller, Phys. Rev. D 2, 2963 (1970).

[5]The examination of LRM has been suggested by S. Nussinov, C. Quigg, and J.-M. Wang [Phys. Rev. D 6, 2713 (1972)] as a way of distinguishing between fragmentation and multiperipheral philosophies.

[6]One can also obtain information useful for distinguishing between classes of models by measuring the amount of charge transfer across the c.m. hemispheres as suggested by T. T. Chou and C. N. Yang [Phys. Rev. D 7, 1425 (1973)]; they give the fragmentation results. The multiperipheral results have been discussed by C. Quigg and G. H. Thomas [*ibid.* 7, 2752 (1973)]. Additional comments on the multiperipheral picture can be found in D. R. Snider, *ibid.* 7, 3517 (1973).

[7]We have given a shortened version of some of these arguments elsewhere; see D. Sivers and G. H. Thomas, this issue, Phys. Rev. D 9, 319 (1974).

[8]An extensive literature exists already on the use of generating functions. We have found the following references useful: A. H. Mueller, Phys. Rev. D 4, 150 (1970); B. R. Webber, Nucl. Phys. B43, 541 (1972); see also Ref. 3(f).

[9]See e.g., C. Quigg, in *Experiments on High Energy Particle Collisions—1973,* Ref. 2, p. 375. The essential point is that the two-particle correlation function C_2 appears energy-independent when $y_1 = y_2 = 0$ (both particles at rest in the c.m. system) over NAL and ISR energies. The fragmentation picture would have $C_2 \propto \sqrt{s}$. Nevertheless the fragmentation picture may still be fair representation of reality at energies below 30 GeV/c and at high energies in the fragmentation region [$x = (2p_L^*/\sqrt{s}) \neq 0$].

[10]C. E. DeTar, Phys. Rev. D 3, 128 (1971). For a review of multiperipheral models see W. R. Frazer, L. Ingber, C. H. Mehta, C. H. Poon, D. Silverman, K. Stowe, P. D. Ting, and H. J. Yesian, Rev. Mod. Phys. 44, 284 (1972).

[11]As far as we know, the idea of a "two-component" model was first used by K. Wilson, Cornell Report No. CLNS-131, 1970 (unpublished).

[12]M. Kac, G. E. Uhlenbeck, and P. C. Hemmer, J. Math. Phys. 4, 216 (1963); 4, 229 (1963); P. C. Hemmer, M. Kac, and G. E. Uhlenbeck, *ibid.* 5, 60 (1964); P. C. Hemmer, *ibid.* 5, 75 (1964).

[13]An introduction to the Bjorken-Feynman-Wilson (BFW) fluid analogy may be found in a set of lectures by R. Arnold [ANL Report No. ANL/HEP 7317, 1973 (unpublished)]. References to the literature and to fluid-theory concepts and their relevance to particle physics can be found therein.

[14]These assumptions have been used previously in the literature. For a discussion and references see D. Sivers and G. H. Thomas, Phys. Rev. D 7, 516 (1973). These assumptions also form the basis of the BFW fluid analog (Ref. 13). Finally, these properties are tacitly assumed for Mueller-Regge-type models for inclusive distributions [Ref. 3(f)].

[15]R. C. Hwa, Phys. Rev. Lett. 26, 1143 (1971); C. Quigg, J.-M. Wang, and C. N. Yang, *ibid.* 28, 1290 (1972).

[16]See Refs. 3(d), 3(f), and 11. The idea of the diffractive contribution changing with energy is discussed in the multiperipheral-model literature in the context of the smallness of the triple-Pomeron coupling times ln$s$ [G. F. Chew and A. Pignotti, Phys. Rev. 276, 2112 (1968)]. The basic exchanges in the model are the Pomeranchuk trajectory and a meson trajectory representing the effect of all lower meson trajectories. To zeroth order the Pomerachuk is not included; its first effect is to determine a high-mass diffractive fragmentation contribution which is small at present energies, but whose effect might become important at higher energies. See, e.g., the discussion of multiperipheral bootstrap models by Frazer *et al.* (Ref. 10) as well as W. R. Frazer, D. R. Snider, and C.-I Tan, Phys. Rev. D 8, 3180 (1973). It will be noted in these references that the multiperipheral-model explanation of diffraction is not without serious conceptual problems, which might be clarified by further experiments.

[17]M. Gell-Mann, Phys. Rev. Lett. 8, 263 (1962); V. N. Gribov and I. Ya. Pomeranchuk, *ibid.* 8, 343 (1962).

[18]T. Kawai, Nuovo Cimento 50A, 176 (1967).

[19]C. E. Jones, F. E. Low, and J. E. Young, Phys. Rev. D 4, 2358 (1971); P. Goddard and A. White, Nuovo Cimento 1A, 645 (1971); C. E. DeTar and J. H. Weis, Phys. Rev. D 4, 3141 (1971).

[20]S.-Y. Mak and C.-I Tan, Phys. Rev. D 8, 4061 (1973); F. Duimio and G. Marchesini, Nucl. Phys. B59, 222 (1973). A proof of equivalence for a general class of models is given by S. Pinsky, D. Snider and G. Thomas [ANL Report No. ANL/HEP 7331, 1973 (unpublished).

[21]This model has been also discussed extensively in terms of the Bjorken-Feynman-Wilson fluid analog; see Arnold (Ref. 13).

[22]Matrix formulation entails some slight changes in Eq. (3.1) (Ref. 16). An example of how isospin is included can be found in D. K. Campbell and S.-J. Chang, Phys. Rev. D 8, 2996 (1973).

[23]Another model giving no left-right correlations is $f(y) = 1 + \lambda\delta(y)$. Then $\bar{f}(\alpha) = 1/\alpha + \lambda$ and $[f(\alpha_R) - f(\alpha_L)]/(\alpha_L - \alpha_R) = 1/(\alpha_L \alpha_R)$, the result in the Chew-Pignotti model. Since the resulting $p(z) = zg/(1 - \lambda zg)$ can give positive f_2 correlations, this model may have some relevance for fitting data. This model and its physical significance will be discussed in detail elsewhere [S. Pinsky, D. Snider, and G. Thomas, ANL Report No.

ANL/HEP 7349, 1973 (unpublished)].
[24]The assumption is that the exchanged t's are small (all less in magnitude than some Δ) in the MPM. This suppresses σ_n for $n > Y/b$ where $\cosh b = 1 + m^2/2\Delta$ and m is some typical resonance mass; see G. Chew and D. R. Snider, Phys. Lett. 31B, 75 (1970).
[25]J. Finkelstein and K. Kajantie, Phys. Lett. 26B, 305 (1968); Nuovo Cimento 56, 659 (1968).
[26]See for example R. C. Brower and J. H. Weis, Phys. Lett. 41B, 631 (1972).
[27]D. R. Snider, Phys. Rev. D 8, 4026 (1973).
[28]J. S. Ball and F. Zachariasen, Phys. Lett. 40B, 411 (1972); 41B, 525 (1972).
[29]The difference between p_+ and the result in Ref. 3(f) is due to the neglect of certain graphs by those authors (see e.g. Ref. 20). We thank S. Pinsky for drawing this to our attention.
[30]Analysis of bubble-chamber data to obtain information on left-right multiplicities has been performed by the following. 205 GeV/c: ANL-NAL collaboration [data presented by J. Whitmore, in *Experiments on High Energy Particle Collisions—1973*, Ref. 2. 12 and 24 GeV/c: Bonn-Hamburg-München collaboration [V. Blobel *et al.*, Hamburg report, 1973 (unpublished)]. 102 GeV/c: T. Ferbel and C. Bromberg (private communication).
[31]G. Bellettini *et al.* (Pisa-Stony Brook collaboration), Phys. Lett. 45B, 69 (1973); and G. Belletini, in *Proceedings of the XVI International Conference on High Energy Physics, Chicago-Batavia, Ill., 1972*, edited by J. D. Jackson and A. Roberts (NAL, Batavia, Ill., 1973), Vol. 1, p. 279.
[32]M. G. Albrow *et al.*, Nucl. Phys. B51, 388 (1973); M. Derrick *et al.*, ANL Report ANL/HEP 7332, 1973 (unpublished).
[33]D. Sivers, Phys. Rev. D 7, 3332 (1973).